

AGGREGATION STUDIES OF THE BETA(34-42) PEPTIDE
AND SYNTHESIS OF TARGETS FOR AMYLOID STAINING AND IMAGING

by

Christopher L. May

B.S. Chemistry, Duke University
(1994)

Submitted to the Department of Chemistry
in Partial Fulfillment of the Requirements for the Degree of

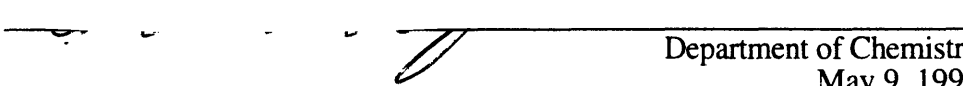
MASTER OF SCIENCE

at the Massachusetts Institute of Technology

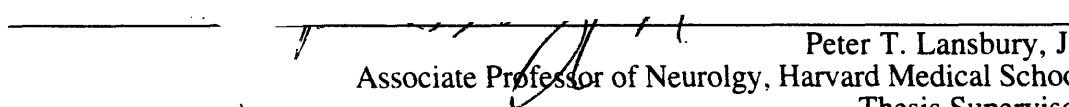
June 1997

© 1997 Massachusetts Institute of Technology
All rights reserved


Signature of Author


Department of Chemistry
May 9, 1997

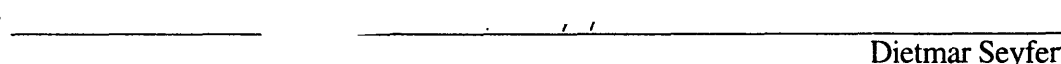
Certified by


Peter T. Lansbury, Jr.
Associate Professor of Neurology, Harvard Medical School
Thesis Supervisor

Certified by


James R. Williamson
Professor of Chemistry
Faculty Advisor

Accepted by


Dietmar Seyferth
Chairman, Departmental Committee on Graduate Students

MASSACHUSETTS INSTITUTE
OF TECHNOLOGY

JUL 14 1997

Science

LIBRARIES

AGGREGATION STUDIES OF THE BETA(34-42) PEPTIDE AND SYNTHESIS OF TARGETS FOR AMYLOID STAINING AND IMAGING

by

Christopher L. May

Submitted to the Department of Chemistry
on May 9, 1997 in Partial Fulfillment of the
Requirements for the Degree of Master of Science

ABSTRACT

Amyloid plaques mostly comprised of variants of the A β protein are hallmarks of the AD brain, and the C-terminus of A β has been identified as an important region for determination of the rate of aggregation of the peptide into fibrils. SSNMR and FTIR studies have suggested an internal framework of hydrogen bonds and hydrophobic interactions which can stabilize the A β fibril and increase the favorability of fibril formation. Replacements of amide bonds in the peptide backbone with esters were synthesized and examined to determine these effects. We present evidence that disruption of the polyamide hydrogen-bond network can alter the kinetic and structural characteristics of the β (34-42) fibril.

Congo red has been used as a stain for amyloid deposits in Alzheimer's disease for the past five decades. Two compounds, based on the core molecule Congo red and a bipyridine-technetium ligand, were designed as possible A β imaging and diagnostic targets. Both are also possible first-generation A β fibrillization inhibitors. Further ideas for a next generation of amyloid inhibitors, based on modifications of functional groups, are also discussed.

Thesis Supervisor: Peter T. Lansbury, Jr.

Title: Associate Professor of Neurology, Brigham and Women's Hospital

Table of Contents

| | |
|---|----|
| List of Illustrations | 4 |
| Acknowledgments | 5 |
| | |
| <u>Chapter I</u> | |
| Kinetic and Structural Analysis of the β(34-42) Peptide | |
| Background | 6 |
| Materials and Methods | 10 |
| Results | 14 |
| Discussion and Summary | 18 |
| References for Chapter I | 21 |
| | |
| <u>Chapter II</u> | |
| Synthesis of a Potential β-Sheet Nucleator and a Spin-Labelled Congo Red Derivative | |
| Background | 23 |
| Materials and Methods | 25 |
| Future Directions | 27 |
| Experimental | 30 |
| References for Chapter II | 34 |
| | |
| <u>Appendix</u> | |
| NMR Spectra | 35 |

List of Illustrations

| | | |
|-------------|---|----|
| 1.1 | The A β amyloid peptide | 7 |
| 1.2: | Two possible orientations of the β (34-42) fibril, and replacement of an amide by an ester in the β -sheet network | 8 |
| 1.3 | Electron microscope scans of β (34-42) and related depsipeptides | 13 |
| 1.4 | Infrared scans of β (34-42) and related depsipeptides | 15 |
| 1.5 | Aggregation runs of β (34-42) and related depsipeptides | 16 |
| 2.1 | Congo red derivatives and bipyridine-peptide synthetic targets | 25 |
| 2.2 | Scheme 1: synthesis of the β -sheet nucleator | 26 |
| 2.3 | Scheme 2: synthesis of the spin-labelled Congo red | 27 |
| 2.4 | Future targets | 29 |
| 2.5 | Scheme 3: prospective synthesis of a Chrysamine G target | 30 |

Acknowledgments

When I first started writing, I thought this would be the easiest section to complete. Now that I'm actually here, I've realized it's actually the hardest. The number of people who have helped me through the past three years is too numerous for me to list them all here, but I have to thank a few people explicitly for their roles in helping me get to this point.

First, I want to thank Peter Lansbury for giving me this project, and allowing me the freedom to run in a direction different from where he first imagined it would go. Sometimes it meant I fell flat on my face, but sometimes I learned a lot more, both about science and myself, than by pursuing an "orthodox" thought path. I am honored to have been able to call him a mentor and friend. Cheon-Gyu Cho, who I worked with in my first years in the group, took my book knowledge of chemistry and turned it into something that was actually useful in the lab. Without him I would never have learned many of the tricks that saved me time, effort, and aggravation. I know Cho's new students in his lab in Korea will learn as much from him as I did.

Kelly and Magdalena, who joined the group with me two years ago, have been a source of strength, humor, and sanity to me throughout my days in the lab. Despite our differences in age and personality, we have struggled through good and bad experiences within the group together. My one regret about leaving is that I won't be here to graduate with both of you. I hope you will continue to be as supportive and caring about each other as you have been to me.

Outside the lab, Deans Isaac Colbert and Margo Thomas provided an outlet for my thoughts, dreams and aspirations. They reminded me that there was more out there at MIT than just the chemistry department, and encouraged me to take advantage of it. Thanks to them, I am leaving the Institute a more thoughtful person than when I came in.

Finally, I want to thank my family for always encouraging my curiosity and sense of adventure, even when most of them didn't have a clue why I was interested. Your support and love has made me who I am today, and will continue to guide me for the rest of my life.

Chapter I

KINETIC AND STRUCTURAL ANALYSIS OF DEPSIPEPTIDE ANALOGS OF THE $\beta(34-42)$ PEPTIDE.

Background

The brains of Alzheimer's disease (AD) victims and Down syndrome patients are characterized by the presence of amyloid plaques, the cores of which are comprised of the 39-43 amino acid β -amyloid protein ($A\beta$), (Figure 1) an alternative splicing product of the amyloid precursor protein.¹⁻⁵ The major components of plaque are the 40- and 42-amino acid isoforms ($\beta(1-40)$ and $\beta(1-42)$, respectively).⁶ Both $\beta(1-40)$ and $\beta(1-42)$ have been shown to aggregate under *in vitro* conditions, and aggregation is characterized by a lag time with little or no increase in fibrillar material followed by a rapid increase in fibril growth, consistent with a nucleation-dependent mechanism.^{7,8} Soluble $\beta(1-42)$ and $\beta(1-40)$ protein have also been found circulating in the cerebrospinal fluid of healthy individuals at nanomolar concentration.⁹ The amount of $\beta(1-42)$ protein has been shown to be dramatically increased in some familial and early-onset AD patients,¹⁰ and $\beta(1-42)$ fibrils have been shown to seed aggregation of $\beta(1-40)$. $\beta(1-42)$ has also been found to be less soluble than $\beta(1-40)$ under *in vitro* conditions.⁷ These results have led to suggestions that the ratio of $\beta(1-42)$ to $\beta(1-40)$ in the brain may be a critical factor in amyloid deposition.^{1,6,11,12}

The synthetic peptide comprising the hydrophobic C-terminus of the $A\beta$ protein, $\beta(34-42)$ (Figure 1), readily forms amyloid fibrils and has been used as a model system for $A\beta$.¹³⁻¹⁵ Since amyloid-forming proteins are typically extremely insoluble and do not readily crystallize, X-ray crystallographic studies are of limited use in probing their structure.¹⁶ As a result, our laboratory

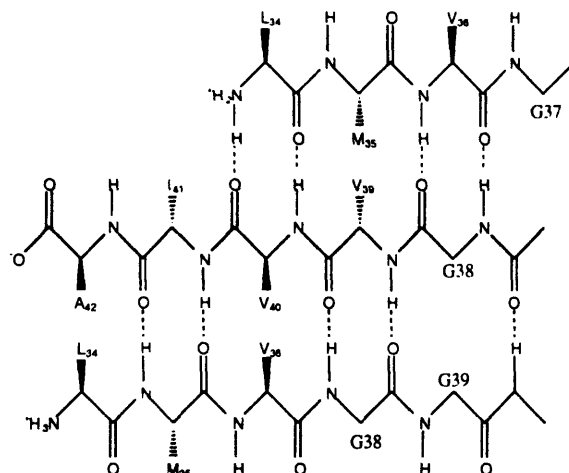
H₂N-DAEFRHDSGYEVHHQKLVFFAEDVGSNKGAIIGLMVGGVVIA-OH

H₂N-Leu-Met-Val-Gly-Gly-Val-Val-Ile-Ala-OH

Figure 1: a) the β -amyloid peptide. The predominant species in AD brain are the 42- and 40-amino acid variants. b) the C-terminus of A β , β (34-42).

has used both FTIR and SSNMR methods for examining the β (34-42) peptide.^{15,17,18} These studies have shown that β (34-42) forms antiparallel β -fibrils which can be observed by electron microscopy.¹³ It was originally believed that there may have been a *cis* -peptide bond between Gly37 and Gly38 in the fibril, however further experiments have shown this to be unlikely^{17,18}. Our model proposes hydrogen-bond contacts are made in one of two discrete patterns between each molecule of β (34-42) and its nearest neighbors. In addition, the hydrophobic side chains seem to be in a close-packing arrangement, with their van der Waals' radii nearly overlapping, excluding water from the system (see Figure 2).¹⁷ In particular, Ile41 and Ala42 are critical to the network, with Ile41 packed against Val39 of the same strand and Met35 of the neighboring strand, and Ala42 surrounded by Val40 of the same strand and Leu34 of the neighboring strand.¹⁷ These hydrophobic interactions offset the entropic costs of trapping the β (34-42) peptide in the amyloid fibril. In each of these models, the polyamide backbone plays a crucial role, either by providing hydrogen bond donors and acceptors, or by limiting the flexibility of side chains. As a result, we became interested in how modifications to the backbone would affect the structure and mechanism of aggregation of the β (34-42) peptide. An understanding of the structural determinants of amyloid aggregation would greatly benefit the search for *in vivo* binders of amyloid as well as inhibitors of amyloid formation, which could be potential AD therapeutics.

a)



b)

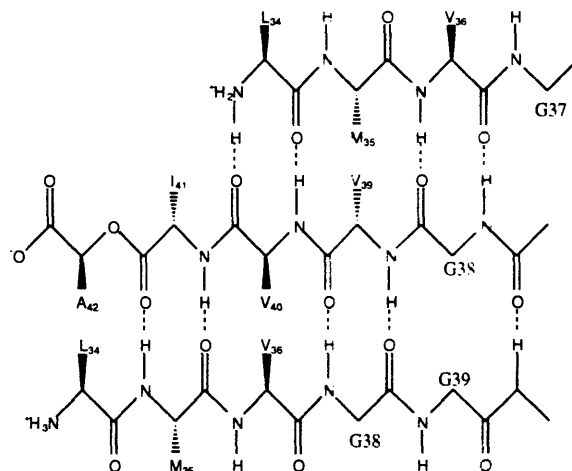
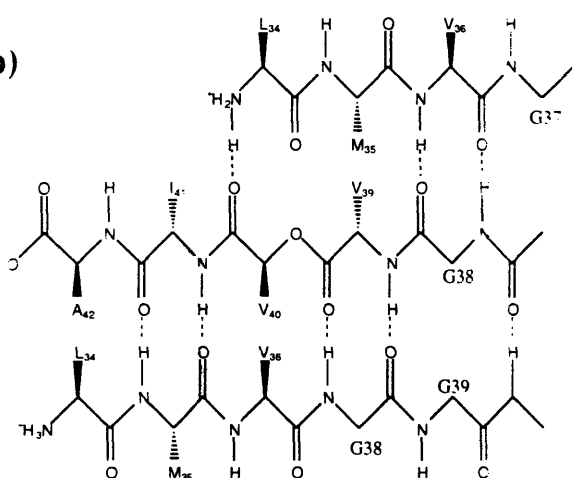


FIGURE 2: a) One possible orientation of the individual peptide strand in the β -sheet of the fibril.¹⁷ b) The β -sheet with one amide replaced by an ester. Note the deletion of an internal hydrogen bond. This interaction would likely be replaced by a water molecule (not shown), which would be entropically expensive. Esters shown are LMVGGV₀VIA and LMVGGVVI₀A.

Bartlett and co-workers¹⁹ and Kent and co-workers²⁰ have replaced the amide backbone in proteins with various functional groups in order to probe the role of the peptide backbone in both structure and function. Thus, measurements of the interaction of the zinc endopeptidase thermolysin with a substrate found a major shift in binding energy upon replacement of a phosphoramidate with a phosphonate ester.¹⁹ These results cannot necessarily be construed as providing the strength of the hydrogen bond interaction, however, due to the difficulty of separating the free energy change due to the hydrogen bond from that due to solvation, as well as non-equivalence of the hydrogen bonds involved.²¹ Depsipeptides have also been shown to have large differences in binding drugs or receptors from their peptide analogs, and several bacteria have been shown to use modifications from amino acids to hydroxy acids, making peptides into depsipeptides, as a method of conveying drug resistance to themselves and their progeny. For example, resistance to vancomycin in *E. faecium* is conferred by the replacement of alanine by lactic acid in a cell-wall dipeptide.²²

With this in mind, we undertook an examination of the effect on aggregation of the replacement of various amide bonds in the $\beta(34-42)$ peptide backbone with esters. Two factors originally influenced our decision: an interest in the earlier Gly-Gly bond measurement, and an interest in disruption of the putative hydrogen-bonding and hydrophobic packing network. The lower barrier to rotation between the cis and trans isomers in the ester versus the amide would presumably provide greater flexibility in the peptide backbone. Our hydrogen-bonding model also suggests deletion of the amide hydrogen bond donor at positions near the C-terminus may disrupt some of the stabilizing contacts predicted to exist in our model of the fibril. Finally, the greater entropic cost of desolvation of the ester and disruption of the hydrophobic interactions stabilizing the fibril would decrease the favorability of the aggregation pathway. Replacements at Gly37 and Val39 were expected to have an effect on aggregation due to their proximity to regions of $\beta(34-42)$ previously shown to be of interest.^{7,14,15,17} We present evidence here that ester replacement can affect on the rate of *in vitro* amyloid formation, and may help to explain the transition of A β from soluble form to aggregate.

Materials and Methods

Synthesis and Purification of Depsipeptides. Peptides β (34-42) and depsipeptides LMVG- Ψ [CO₂]-GVVIA (G₀G), LMVGG- Ψ [CO₂]-VVIA (G₀V), and LMV- Ψ [CO₂]-GGVVIA (V₀G) were synthesized manually on the Wang resin using standard Fmoc chemistry. The ester linkages were prepared by coupling the corresponding hydroxy acid to the resin-bound peptide using standard solid-phase peptide synthesis techniques, then forming the ester by addition of the next Fmoc-amino acid (3 eqs.) with diisopropylcarbodiimide (3 eqs.) and dimethylaminopyridine (5 eqs.) and coupling on the resin for 24 h.^{23,24} Depsipeptides LMVGGV- Ψ [CO₂]-VIA (V₀V) and LMVGGVVI- Ψ [CO₂]-A (I₀A) were manually synthesized on Kaiser oxime resin using Boc protocols;^{25,26} in these cases, Boc-Val- Ψ [CO₂]-Val-OH and Boc-Ile- Ψ [CO₂]-Ala-OH were synthesized according to a published procedure²⁷ and added to the resin as a single unit. Boc-Val- Ψ [CO₂]-Val-OH was in accordance with earlier reported literature values.²⁸ Peptides were cleaved from the resin with N-hydroxypiperidine and the C-terminus converted to the free acid with zinc and 90% aqueous acetic acid.¹⁵ The filtrates were concentrated, and the depsipeptides precipitated

| | R _t (min.) | Gly (exp.) | Ala | Val | Met | Ile | Leu |
|------------------|-----------------------|------------|---------|---------|---------|---------|---------|
| V ₀ G | 29.30 | 1.2 (1) | 1.2 (1) | 2.3 (2) | 0.7 (1) | 1.1 (1) | 1.6 (1) |
| G ₀ G | 21.42 | 1.2 (1) | 1.2 (1) | 2.1 (3) | 0.8 (1) | 1.0 (1) | 1.7 (1) |
| G ₀ V | 16.66 | 1.3 (1) | 1.1 (1) | 2.6 (2) | 0.7 (1) | 1.0 (1) | 1.7 (1) |
| V ₀ V | 17.44 | 2.1 (2) | 1.2 (1) | 2.0 (2) | 0.6 (1) | 1.0 (1) | 1.1 (1) |
| I ₀ A | 17.53 | 2.4 (2) | N/A | 2.1 (3) | 0.7 (1) | 1.1 (1) | 1.8 (1) |

Table 1: Retention volumes and amino acid analyses for depsipeptides V₀G, G₀G, G₀V, V₀V, and I₀A (amino acid analysis based on leucine).

by the dropwise addition of cold H₂O. Precipitates were collected by centrifugation, washed with water and lyophilized. Peptides were dissolved in HFIP and purified by RP-HPLC on a C4 column (5 min. 90% water with 0.1% TFA/10% 5:95 trifluoroethanol:acetonitrile, 5 min gradient to 80:20, 20 min gradient to 70:30, see Table 1 for retention volumes). Peptides were analyzed by PD-MS or FAB-MS (Quality Controlled Biochemicals). Purity was greater than 90% as judged by analytical RP-HPLC (85% water with 0.1% TFA/15% 5:95 trifluoroethanol:acetonitrile). Mass spectrometry: β (34-42): 876.2, 860.3(M⁺); V₀G: 875.3, 860.1(M⁺), 811.0, 786.0; G₀G: 876.2, 860.1(M⁺), 814.8, 784.9; G₀V: 874.0, 859.3(M⁺), 830.8, 600.2; V₀V: 859.8(M⁺); I₀A: 859.9(M⁺).

Boc-L-isoleucyl-L- α -lactic acid benzyl ester. To a solution of L- α -lactic acid benzyl ester (7.58 g, .042 mol), dimethylaminopyridine (.531 g, 4.35 mmol) and Boc-L-isoleucine-OH (12.16 g, .051 mol) in dichloromethane (40 ml) was added diisopropylcarbodiimide (6.58 ml, .042 mol). The solution was allowed to stir for 4 hours at RT, the urea precipitate filtered off and the solvent removed in vacuo to yield a yellow-white gum. The residue was chromatographed on silica gel (8:92 ethyl acetate:hexane) to afford the product, Boc-L-isoleucyl-L- α -lactic acid benzyl ester (10.82 g, 65%). ¹H NMR(300 MHz, CDCl₃): δ 7.36 (s, 5 H), 5.19 (dd, 1 H, J₁ = 7.2 Hz, J₂ = 5.7 Hz), 5.18 (s, 2 H), 5.12 (d, 1 H, J = 5.7 Hz), 4.36 (q, 1 H, J = 4.2 Hz), 1.54 (d, 3 H, J = 6.6 Hz), 1.47 (s, 9 H), 1.20 (m, 1 H), 0.99-0.89 (m, 8 H); ¹³C NMR(300 MHz, CDCl₃): δ 171.82 (Boc C=O), 170.17 (COOBn), 155.54 (int. C=O), 128.55, 128.46, 128.39, 128.17 (phenyl), 79.72 (C t-butyl), 69.10 (O-CH), 66.96 (O-CH₂), 57.64 (N-CH), 37.85 (isoleucyl CH), 28.25 (t-butyl), 24.52 (CH-CH₂), 16.92 (lactyl CH₃), 15.21 (CH₃-CH), 11.56 (CH₃-CH₂).

Boc-L-isoleucyl-L- α -lactic acid. Boc-L-isoleucyl-L- α -lactic acid benzyl ester (10.79 g, .027 mol) was dissolved in methanol and hydrogenated in the presence of 10% Pd/C for 4.5 hours. The resultant solution was filtered through Celite, and concentrated to the product, Boc-L-isoleucyl-L- α -lactic acid, as a white solid (4.666 g, 56%). ¹H NMR(300 MHz, CDCl₃): δ 6.32

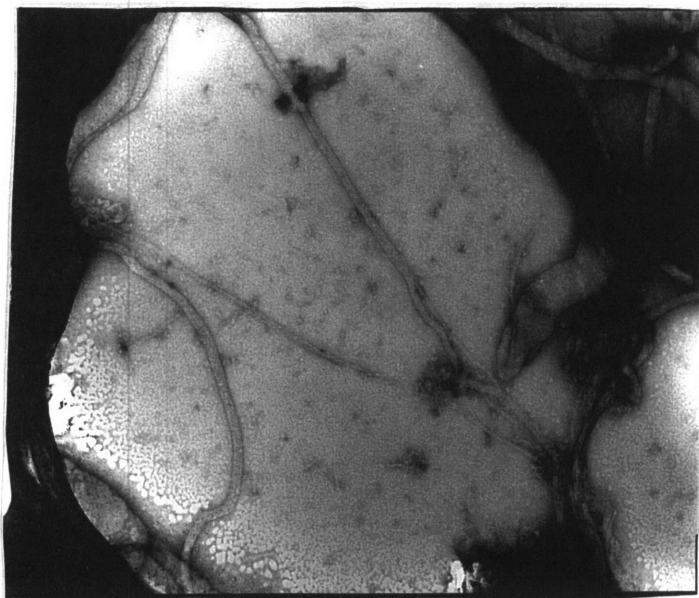
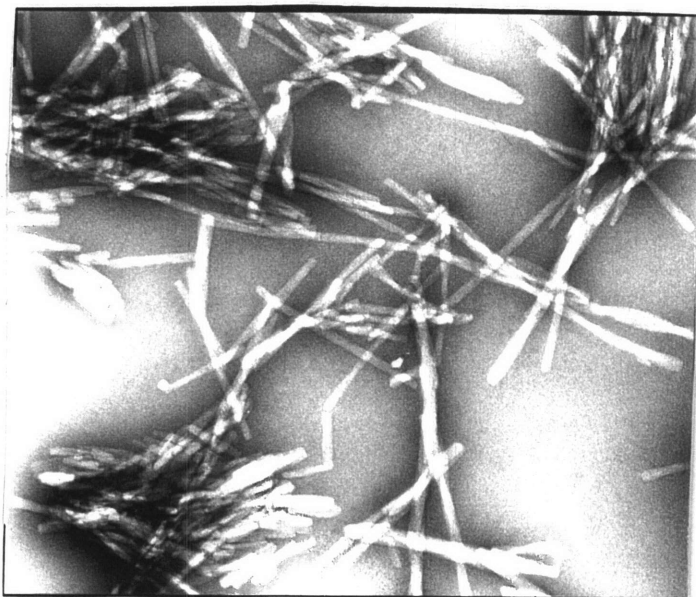
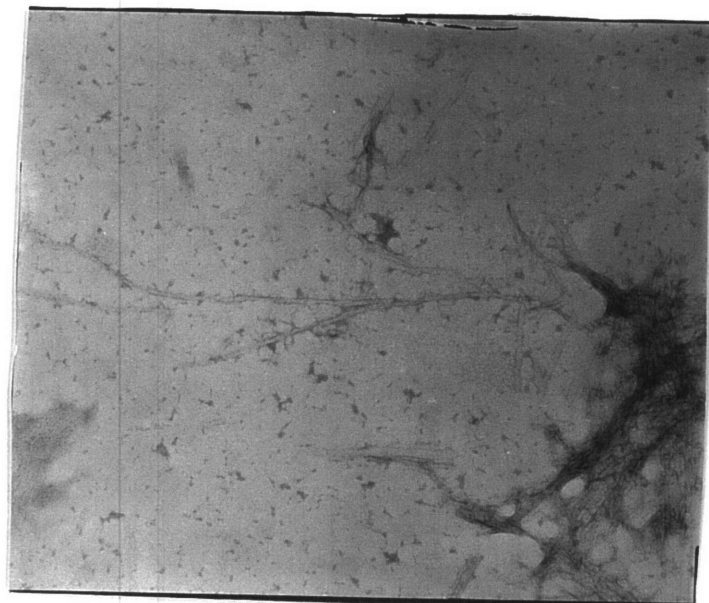
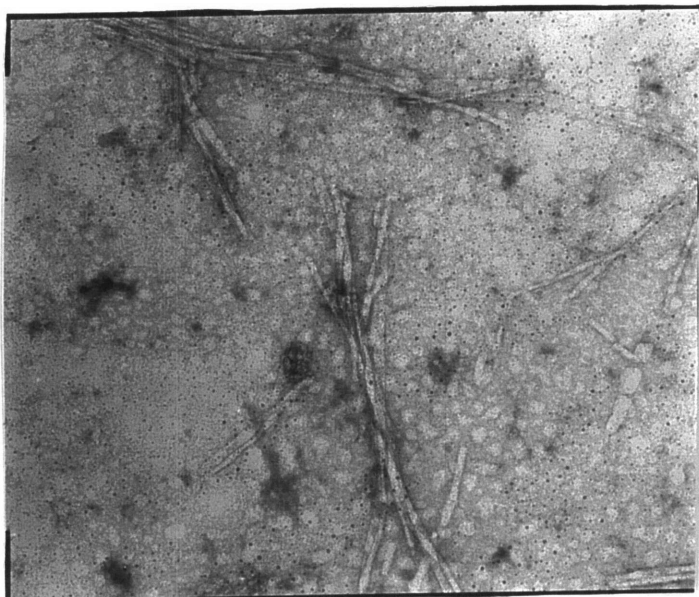
(d, 1 H, $J = 6.8$ Hz), 5.12 (m, 2 H), 4.31 (dd, 1 H, $J_1 = 4.3$ Hz, $J_2 = 8.8$ Hz), 4.09 (m, 1 H), 1.52 (d, 3 H, $J = 8.8$ Hz), 1.42 (s, 9 H), 1.15 (m, 2 H), 0.96 (d, 3 H, $J = 7.0$ Hz), 0.89 (t, 3 H, $J = 7.3$ Hz); ^{13}C NMR(300 MHz, CDCl_3): δ 175.34 (Boc C=O), 171.97 (COOH), 155.90 (int. C=O), 80.11 (C t-butyl), 68.78 (O-CH), 57.84 (N-CH), 37.85 (isoleucyl CH), 28.34 (t-butyl), 24.49 (CH-CH₂), 16.92 (lactyl CH₃), 15.41 (CH₃-CH), 11.65 (CH₃-CH₂).

Electron Microscopy. Depsipeptides aggregated as described above were suspended on carbon-coated copper grids and stained with 2% (w/v) uranyl acetate. Pictures were taken using a JEOL 100-S electron microscope at 80 kV.

FTIR Spectroscopy. Suspensions of amyloid fibrils formed as described above were centrifuged to remove DMSO and buffer, washed and resuspended in water, then dried on a CaF₂ plate. Spectra were recorded on a Perkin-Elmer 1600 series FTIR spectrophotometer. For each sample a 64-scan interferogram was accumulated and averaged, and the contribution from air subtracted.

Kinetic Aggregation Studies. Stock solutions were prepared by dissolving peptide in DMSO, and the concentration determined by amino acid analysis (MIT Biopolymers Laboratory, see Table 1). Solutions (typically 10-15 mM in peptide) were vacuum frozen and thawed under argon to minimize oxidation of methionine. Due to the tendency of the peptides to aggregate in DMSO after 2-3 weeks in solution, all stocks were used immediately upon preparation.²⁹ Aliquots of stock solution were added to an aqueous buffer (100 mM NaCl, 10 mM NaH₂PO₄, pH 7.4), and the turbidity at 400 nm was measured on a Hewlett-Packard 8452a UV spectrophotometer, with scans taken every 195.1 seconds. In order to minimize the effect of DMSO on the solubility of the

Figure 3 (facing page): EM photographs of (from top, left to right): a) β (34-42), b) LMV₀GGVVIA, c) LMVG₀GVVIA, d) LMVGG₀VVIA, e) LMVGGVVI₀A. Periodic higher deposition of staining shows the fibril twist in scans c) and e). Photos shown are representative images from a number of scans. The scale for all scans is 100 nm.



peptide, the stock solution was limited to less than 10% of the final volume. Fibrils were suspended by stirring the solution at 1440 rpm between measurements. To minimize the effects of stirring on the light scattering measurements, stirring was stopped for 7.5 seconds before and after each measurement. Data from two to three identical experiments were averaged to provide final data (error in each data point = $\pm 10\%$).

Solubility Measurements. Depsipeptide solutions from aggregation studies were placed in an aqueous buffer described above, stirred at 1440 rpm for 24 hours, then incubated by standing at room temperature for at least two weeks, then centrifuged at 14,000 rpm for 5 minutes and filtered (Millipore HV 0.45 μm filters) to remove aggregate. Concentrations were determined by amino acid analysis as above and quantitative ninhydrin test.²⁵

Results

Electron microscope photographs are shown in Figure 3. EM scans of depsipeptide fibrils generally showed two types of assemblies: fibrils with a diameter of approximately 2.5 nm and variable length, ranging from 25-100 nm, and slightly thicker twisted fibrils.¹³ There were few differences between depsipeptides and $\beta(34-42)$ with the exception of I₀A, which seemed to be composed of larger rope-like bundles of fibrils 5 nm in diameter and 70 nm in length. These morphological differences may be responsible for the difficulty of accurately measuring the aggregation profile of I₀A (see below).

FTIRs for all depsipeptides and $\beta(34-42)$ are shown in Figure 4. In all cases, a strong peak can be seen at $\sim 1630\text{ cm}^{-1}$, indicative of the amide I stretch in a β -sheet conformation, and a medium peak between 1530 and 1550 cm^{-1} corresponds to the amide II stretch.^{30,31} The amide I stretches of the depsipeptides are shifted downfield by $4-6\text{ cm}^{-1}$ compared to those of $\beta(34-42)$. In addition, $\beta(34-42)$ shows an additional weak stretch at 1698 cm^{-1} , indicative of the antiparallel β -sheet, in accordance with earlier results.¹⁵ None of the depsipeptides show this peak before or after

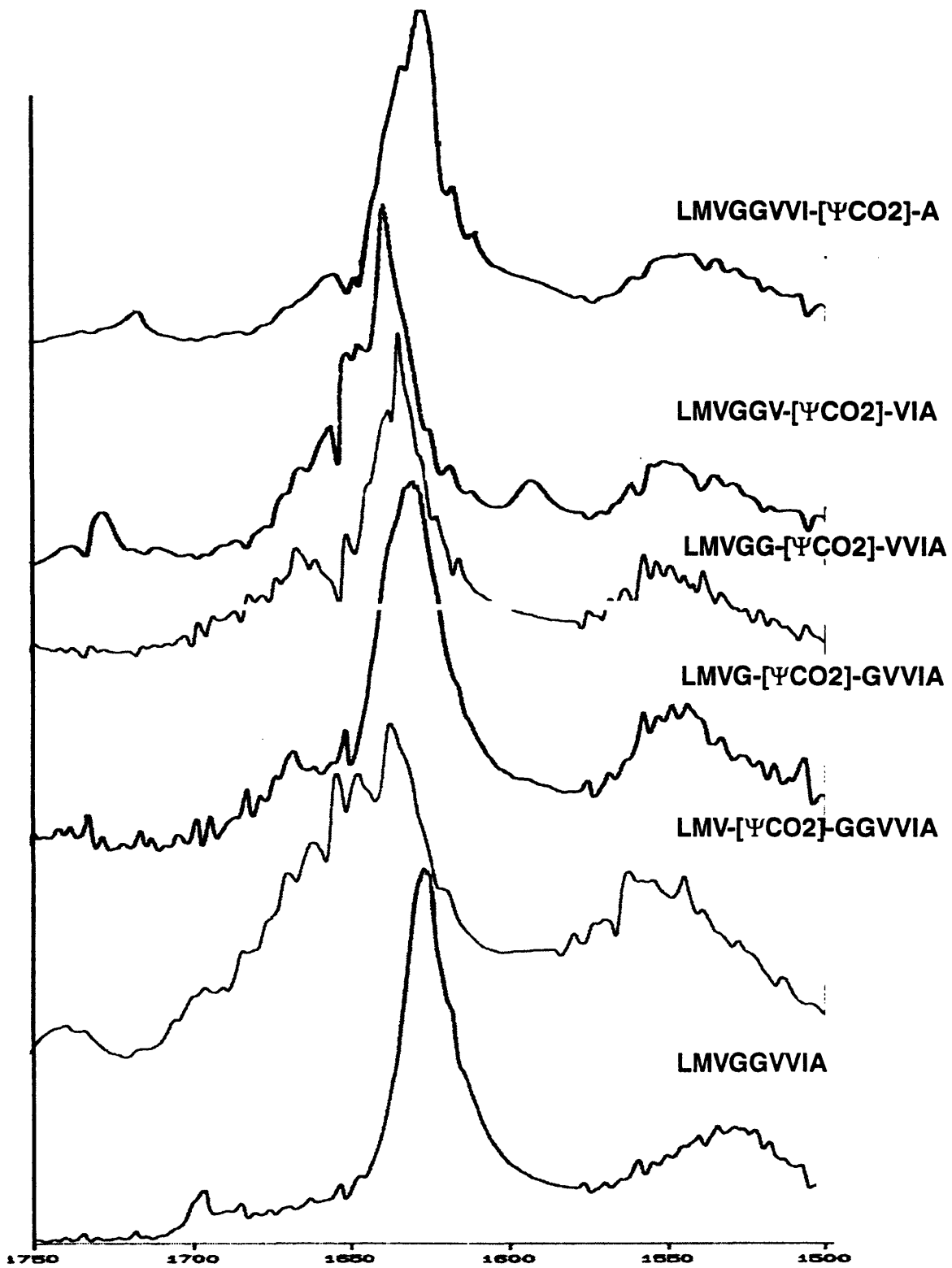


Figure 4: Infrared scans of $\beta(34-42)$ and related decapeptide fibrils.

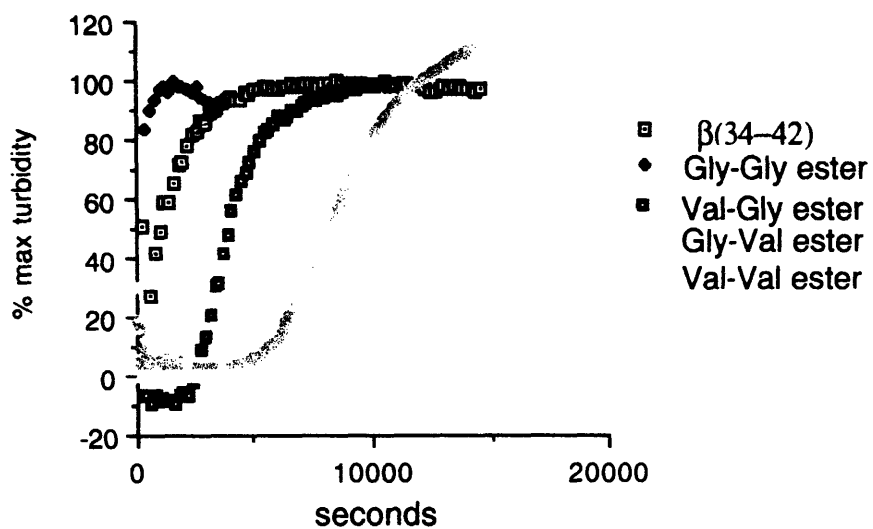


FIGURE 5: Kinetic aggregation curves of $\beta(34-42)$ and depsipeptides at $375 \mu\text{M}$. All runs were performed in triplicate at 1440 rpm. Scans were taken every 195.1 seconds. Raw data was averaged over all three runs then normalized to 100% maximum turbidity for each peptide. Standard deviations for each peptide are represented by error bars.

deconvolution of their spectra. All depsipeptides have absorbances between 1715 and 1730 cm^{-1} representing the ester stretch.

A comparison of kinetic aggregation data is shown in Figure 5. In general, at 375 μM , depsipeptides showed few deviations from the aggregation profile of "native" $\beta(34-42)$. However, at 375 μM , V_0V remains soluble in buffer for at least 2 weeks, the maximum period of time light scattering was measured. V_0V does aggregate at higher concentrations (~ 2 mM), where lag times are approximately 30,000 seconds. For an identical concentration of peptide, G_0G was found to reach maximum turbidity in approximately one-half the time of $\beta(34-42)$ (see Figure 1). This may be due to an inherent flexibility in the ester bond of the G_0G peptide which is not present in the amide bond of $\beta(34-42)$, allowing it to more quickly sample the (or a) conformation necessary for aggregation, which then traps the peptide in the fibril. Alternatively, G_0G may simply possess the necessary conformation, or a near neighbor, as its most stable form in solution. Absolute turbidity measurements varied from peptide to peptide, as expected unless the fibrils formed from various depsipeptides were absolutely similar.

Final solubilities of all peptides are shown in Table 2. As can be seen there is a clear trend for solubility to increase as lag time increases, though not in a linear manner. Peptides G_0G , V_0G .

TABLE 2. Final Solubilities of $\beta(34-42)$ and Depsipeptides

| Peptides | Final Solubility (μM) |
|--------------------------|------------------------------------|
| LMVGGVVIA | 25 ± 5 |
| LMV ₀ GGVVIA | 28 ± 8 |
| LMVG ₀ GGVVIA | 26 ± 6 |
| LMVGG ₀ VVIA | 76 ± 16 |
| LMVGGV ₀ VIA | > 1000 |
| LMVGGVVI ₀ A | 129 ± 36 |

and $\beta(34-42)$ either have no or negligible lag times, and their final solubilities are indistinguishable from one another. These numbers cannot be considered the thermodynamic solubility of the depsipeptides, since the analogous reverse solubilization experiments were not performed.

Previous experiments have suggested that the replacement of an amide-carbonyl interaction by that of an ester-carbonyl has a ΔG of from 0.5 to 1.8 kcal/mol²¹ or 4.0 kcal/mol.¹⁹ This would imply a corresponding 1.6 to 54.5- fold increase in K_{SP} based solely on alteration of the amide, if it indeed stabilizes the fibril via an amide-carbonyl interaction. Compared to $\beta(34-42)$, G_OV , V_OV , and I_OA all fall within this range, with V_OV in particular appearing at the far end of the range, approximately 50-fold less soluble than $\beta(34-42)$.

Earlier experiments in our laboratory⁷ have shown that both $\beta(1-42)$ and NAC are capable of seeding formation of the $\beta(1-40)$ fibril. To determine if depsipeptides with an extended lag time could interfere with the aggregation of $\beta(34-42)$, we mixed stock solutions of G_OG , I_OA , and V_OV with $\beta(34-42)$ stock in a 10:90 ratio, then ran the new solutions in accordance with our aggregation protocol. In all cases, there was no discernible alteration of the $\beta(34-42)$ aggregation curve (data not shown).

Discussion

At present, it is unknown whether aggregated $A\beta$ is made up of a single conformer or occupies a number of energetically similar states. Experiments recently performed have suggested that the Gly37-Gly38 amide bond is in the *trans*- conformation.¹⁸ Given the preference of the ester for the E- as opposed to Z-isomer, and previous results suggesting that the central glycine residues may not be part of the β -sheet, the faster aggregation of G_OG may be due to simple hydrophobic effects of an ester versus an amide. In this model, the amide proton between Gly37 and Gly38 is solvated in the fibril as well as free in solution, thus replacement of the amide by an ester would cause no net entropic loss. In the case of Val39, it is possible that the peptide requires relative rigidity at this

position for rapid formation of the fibril. The barrier to rotation about the C-O bond in the ester has been calculated as ~10-15 kcal/mol, versus 20 kcal/mol for amides³²⁻³⁴. Perhaps the cis-amide conformation is necessary as a nucleator of aggregation, but is not the most stable conformer in the fibril itself. By this model, once the seed is formed, cis/trans isomerization takes place and favors the lower energy conformer. It is also possible that the depsipeptides may take on an entirely different secondary and tertiary structure from the native peptide. In this case, the different lag times for the depsipeptides with respect to $\beta(34-42)$ may be a result of differences in packing efficiency versus a standard β -sheet within the fibril.

The mixed ester experiments show no inhibitory effect or enhancement of depsipeptides on aggregation, at least for $\beta(34-42)$. Either the two peptides follow totally independent aggregation processes in which the native and depsipeptides each form their own, homogeneous, fibrils, or the incorporation of the slower (or faster) aggregating depsipeptides into the $\beta(34-42)$ fibril does not appreciably affect the aggregation pathway of the native peptide.

Previous FTIR experiments in our laboratory have suggested that Val36, Val39, and Val 40 are important residues in the model β -sheet on the basis of a frequency shift in ^{13}C -labeled $\beta(34-42)$.¹⁵ In these experiments the amide I stretch of a ^{13}C -labeled carbonyl and its nearest neighbors is shifted downfield based on energy transfer within the β -sheet.¹⁵ Ester "labelling" should function on a similar basis, with the amide I stretch of the sheet being displaced downfield, although by a minor amount compared to ^{13}C -labelling. This work confirms the expectations of the previous model, with perturbations at these three positions having an effect on the aggregation rate, and therefore formation of the β -sheet in the fibril. In particular, the ester between Val39 and Val40 should have a major effect, as it disrupts two of the four critical residues, a prediction borne out by our results. Similarly, the central glycine residues are predicted to not be a part of the β -sheet structure, and so perturbation should not have a negative effect on the formation of the fibril.

The depsipeptide I₀A was difficult to measure, possibly due to the macroscopic properties of its fibril. Whereas the other depsipeptides studied in this series aggregated in fibrils which could be easily suspended for turbidity measurements, I₀A tended to aggregate into "clump" fibrils which

would immediately sediment at the spin rates used. This was confirmed in the EM scans, which showed the I₀A fibril to be much thicker than those of other depsipeptides (see above). Previous experience in our lab has shown that the turbidity assay is very sensitive to changes in the stirring rate of the solution³⁵. Thus, the kinetic data for I₀A may not be directly comparable to that of other depsipeptides.

Summary

This work has shown that seemingly minor alterations in the structure of a model A β peptide can potentially have a major effect on its rate of aggregation and final solubility by disruption of the hydrogen-bond structure and hydrophobic interactions of the β -sheet. In addition, such changes can also affect the structure of the fibril itself, once formed. It is still unknown exactly how the individual A β peptides come together and self-organize to form the fibril. Further work in this area should help to elucidate the structural requirements necessary for fibrillar formation, and point the way towards possible therapeutics aimed at slowing or reversing the aggregation process.

References for Chapter I

- (1) Harper, J.D.; Lansbury, P.T., Jr. *Ann. Rev. Biochem.* **1997** *66* , 385-407
- (2) Selkoe, D. *J. NIH Research* **1995** *7* , 57-64
- (3) Kang, J.; Lemaire, H.-G.; Unterbeck, A.; Salbaum, J.M.; Grzechik, K.-H.; Multhaup, G.; Beyreuther, K.; Muller-Hill, B. *Nature* **1987** , 733-736
- (4) Katzman, R.; Saitoh, T. *The FASEB J.* **1991** *5* , 278-286
- (5) Masters, C.L.; Simms, G.; Weinman, N.A.; Multhaup, G.; McDonald, B.L.; Beyreuther, K. *Proc. Natl. Acad. Sci. U.S.A.* **1985** *82* , 4245
- (6) Lansbury, P.T., Jr. *Acc. Chem. Res.* **1996** *29* , 317-321
- (7) Jarrett, J.T.; Berger, E.P.; Lansbury, P.T., Jr. *Biochem.* **1993** *32* , 4693-4697
- (8) Iverson, L.L.; Mortishire-Smith, R.J.; Pollack, S.J.; Shearman, M.S. *Biochem. J.* **1995** *311* , 1-16
- (9) Seubert, P.; Vigo-Pelfrey, C.; Esch, F.; Lee, M.; Dovey, H.; Davis, D.; Sinha, S.; Schlossmacher, M.; Whaley, J.; Swindlehurst, C.; McCormack, R.; Wolfert, R.; Selkoe, D.; Lieberburg, I.; Schenk, D. *Nature* **1992** *359* , 325
- (10) Suzuki, N.; Cheung, T.T.; Cai, X.-D.; Odaka, A.; Otvos, L., Jr.; Eckman, C.; Golde, T.E.; Younkin, S.G. *Science* **1994** *264* , 1336-1340
- (11) Kosik, K.S. *J. Cell Biol.* **1994** *127* , 1501-1504
- (12) Bush, A.I.; Beyreuther, K.; Masters, C.L. *Pharmac. Ther.* **1992** *56* , 97-117
- (13) Halverson, K.; Fraser, P.E.; Kirschner, D.A.; Lansbury, P.T., Jr. *Biochem.* **1990** *29* . 2639-2644
- (14) Spencer, R.G.S.; Halverson, K.J.; Auger, M.; McDermott, A.E.; Griffin, R.G.; Lansbury, P.T., Jr. *Biochem.* **1991** *30* , 10382-10387
- (15) Halverson, K.J.; Sucholeiki, I.; Ashburn, T.T.; Lansbury, P.T., Jr. *J. Am. Chem. Soc.* **1991** *113* , 6701-6703
- (16) Lotz, B.; Gonthier-Vassal, A.; Brack, A.; Magoshi, J. *J. Mol. Biol.* **1982** *156* , 345

- (17) Lansbury, P.T., Jr.; Costa, P.R.; Griffiths, J.M.; Simon, E.J.; Auger, M.; Halverson, K.J.; Kocisko, D.A.; Hendsch, Z.S.; Ashburn, T.T.; Spencer, R.G.S.; Tidor, B.; Griffin, R.G. *Nature Struct. Bio.* **1995** *2*, 990-998
- (18) Costa, P.R.; Kocisko, D.A.; Sun, B.Q.; Lansbury, P.T., Jr.; Griffin, R.G. *J. Am. Chem. Soc.* **1997** *in publication*,
- (19) Bartlett, P.A.; Marlowe, C.K. *Science* **1987** *235*, 569-571
- (20) Schneider, M.; Kent, S.B.H. *Science* **1992** *256*, 221-225
- (21) Fersht, A.R. *Trends Biochem. Sci.* **1987** *12*, 30-34
- (22) Bugg, T.D.H.; Wright, G.D.; Dutka-Malen, S.; Arthur, M.; Courvalin, P.; Walsh, C.T. *Biochem.* **1991** *30*, 10408-10415
- (23) Merrifield, R.B. *J. Am. Chem. Soc.* **1963**,
- (24) Erickson, B.W.; Merrifield, R.B. *J. Am. Chem. Soc.* **1973** *95*, 3750-56
- (25) Degrado, W.F.; Kaiser, E.T. *J. Org. Chem.* **1980** *45*, 1295
- (26) Degrado, W.F.; Kaiser, E.T. *J. Org. Chem.* **1982** *47*, 3258
- (27) McLaren, K.L. *J. Org. Chem.* **1995** *60*, 6082-6084
- (28) Dory, Y.L.; Mellor, J.M.; McAleer, J.F. *Tetrahedron* **1996** *52*, 1343-1360
- (29) Evans, K.C.. Conformational Studies of the Beta Amyloid Protein and *In Vitro* Models for the Effect of Apolipoprotein E on Fibril Formation in Alzheimer's Disease, *Ph.D. Thesis, Massachusetts Institute of Technology*, **1996**.
- (30) Susi, H.; Byler, D.M. *Methods Enzymol.* **1986** *130*, 290-311
- (31) Krimm, S.; Bandekar, J. *Adv. Protein Chem.* **1986** *38*, 181-364
- (32) Blom, C.E.; Gunthard, H.H. *Chem. Phys. Lett.* **1981** *84*, 267
- (33) Grindley, T.B. *Tetrahedron Lett.* **1982** *23*, 1757-1760
- (34) Wiberg, K.B.; Laidig, K.E. *J. Am. Chem. Soc.* **1987** *109*, 5935-5943
- (35) Evans, K.C.; Berger, E.P.; Cho, C.-G.; Weisgraber, K.H.; Lansbury, P.T., Jr. *Proc. Natl. Acad. Sci. USA* **1995** *92*, 763-767

Chapter II

SYNTHESIS OF A POTENTIAL β -SHEET NUCLEATOR AND A SPIN-LABELLED CONGO RED DERIVATIVE.

Background

One of the great difficulties of clinical research and treatment of Alzheimer's disease is the inability to monitor the disease progress in a living being. To date, only a probable diagnosis of AD can be made via cognitive and physical examinations; confirmation can only be achieved upon autopsy by examination of the brain for amyloid plaque. If it were possible to follow the time course of brain amyloid deposition in a person suffering from AD, it would provide many answers about the time course and correlation of neurodegenerative events in the brain.

One of the most common methods used for identifying dense (but not diffuse) Alzheimer's amyloid plaque is staining with the dye Congo red, which induces a green birefringence upon binding.¹ Indeed, the classic definition of amyloid is stated in terms of birefringent staining with Congo red. The method of binding between Congo red and $A\beta$ is unknown, but is believed to involve intercalation of the π system of the naphthyl and biphenyl rings with the hydrophobic side chains of the $A\beta$ C-terminus. Recent work in our lab^{2,3} has involved designing and studying various analogs of Congo red and other dyes, such as Chrysamine G, in an attempt to determine what portions of the molecule are important for binding to amyloid. Small changes in the structure of Congo red was found to have major effects on the binding affinity of the dye to IAPP^H, a pancreatic amyloid.² Thus, we have theorized that different dye analogs may bind the various isoforms of $A\beta$ with different selectivities, allowing the eventual design of a dye which can selectively bind $A\beta(1-42)$ while leaving $A\beta(1-40)$ free.

Recent work by Kelley^{4,5} and co-workers has focused on flexible "templates" comprising peptides linked by an aromatic diacid or diamine which could be used to induce a peptide into a β -sheet conformation. In the β -sheet example, these templates function by capturing a free peptide between two complementary peptide strands with a high propensity for β -sheet formation. The aromatic portion of the template can serve two functions: as a "spacer" and link to keep the two complementary strands the proper distance necessary for interstrand hydrogen bonds to potentially form between them and the free peptide, and as a potential metal binder for transition metals such as copper or zinc, which can then chelate the carboxylate moiety of the free peptide strand.

Our laboratory has recently focused on the design of small molecule compounds capable of binding technetium which show the potential for blood-brain barrier transport as possible imaging agents for amyloid in AD brain.³ Due to the high affinity of technetium for nitrogen, one of our earliest experiments was the replacement of the biphenyl ring in Congo red with a bipyridyl, followed by chelation of the bipyridyl nitrogens with technetium via reaction with ammonium pertechnetate. Other experiments led us to create an analog of Congo red with an aminomethyl handle for attachment of other compounds, such as dyes and metal binders, to use Congo reds affinity for amyloid to bring other molecules which can be measured spectroscopically into the vicinity of the amyloid fibril. As a result, our synthetic efforts focused in two parallel directions. In one case, we used a bipyridine diacid linked to two truncated C-terminal A β peptides as a model compound for sequestration of A β . The bipyridine was chosen as a spacer due to the possibility of later introducing metals as chelating agents into the molecule. In the other, our handled Congo red molecule was used to attach a nitroxide free radical (3-carboxy PROXYL, **11**) to the dye, thus using the Congo red analog as a potential spin label for electron spin resonance (ESR) studies.

In sum, the goal of our synthetic efforts was twofold. In the case of peptidomimetic

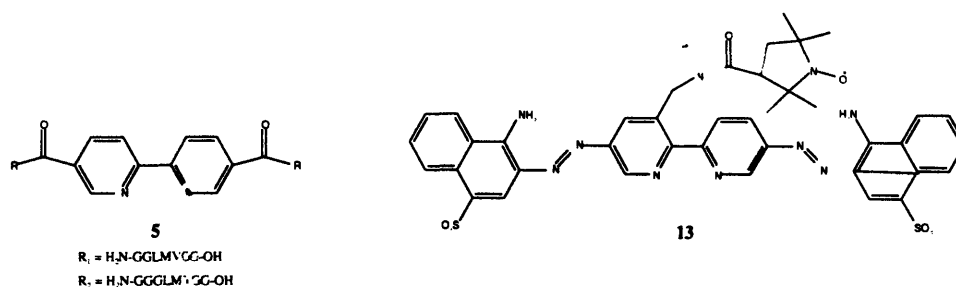


Figure 1: Congo red derivatives and bipyridine-peptide synthetic targets.

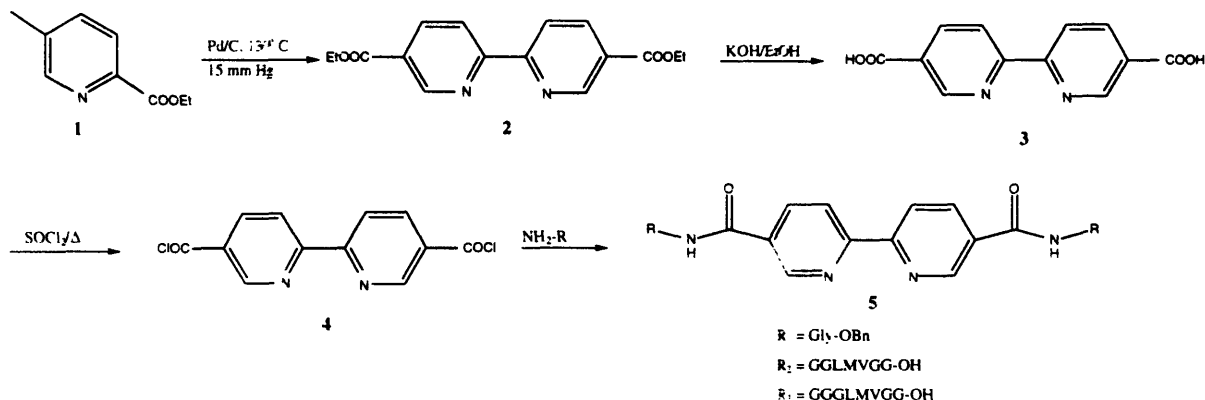
compound **5**, our goal was to develop first-generation compounds capable of binding a molecule of A β via a "trap" into the β -sheet conformation. Theoretically, this molecule could also act as a sequestration agent for A β , by limiting the interaction of individual Ab peptides with one another. In the case of spin-labelled Congo red analog **13**, our goal was to determine in more detail, via electron spin resonance, the method of binding between a molecule of Congo red and the A β amyloid fibril.

Materials and Methods

Synthesis of a Potential β -Sheet Nucleator. Our aromatic diacid linker **4** was synthesized via commercially available ethyl nicotinate **1** (see Scheme 1), which was converted to 2,2'-bipyridyl-5,5'-diethyl dicarboxylate by a known procedure,⁶ then hydrolyzed in KOH/EtOH to the diacid in quantitative yield. Diacid **3** was insoluble in all solvents and difficult to work with, so diacid chloride **4** was made via refluxing overnight in thionyl chloride.⁷ This material which was used in the coupling step.

Peptides H₂N-GGLMVGG-OH and H₂N-GGGLMVGG-OH were prepared by standard Fmoc coupling techniques on Wang resin. Purification was performed on a C18

Scheme 1

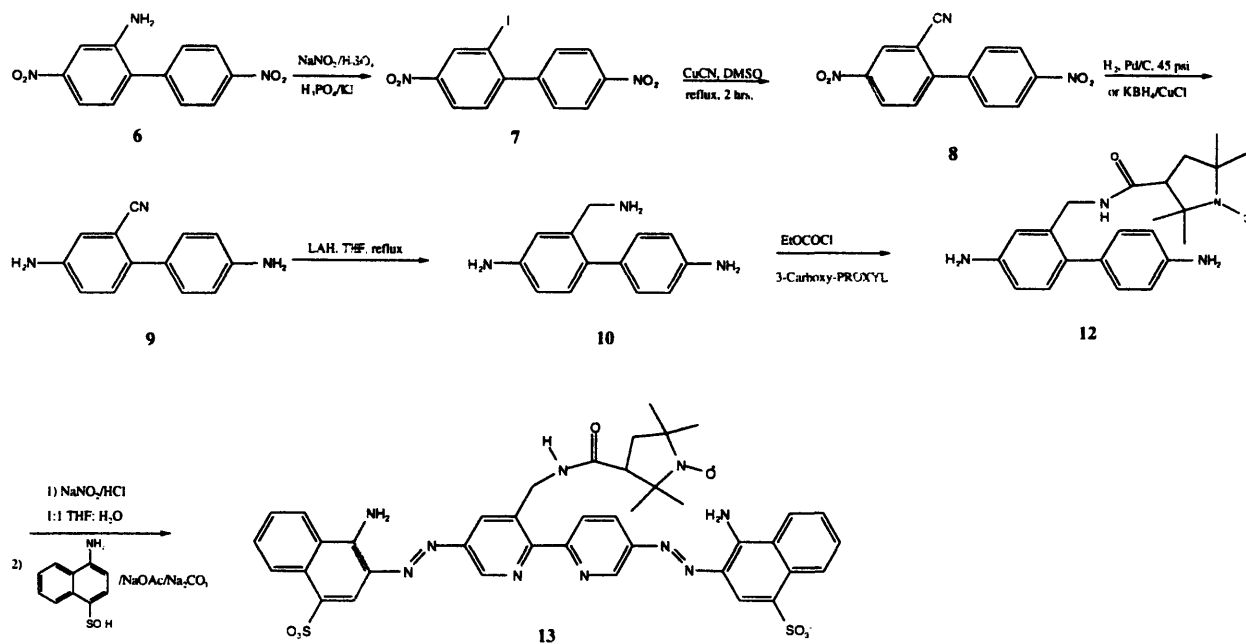


column (100% water for 5 min., then 40 min. gradient 100% water to 80:20 water:acetonitrile, retention time = 38 min.) Purified peptides were confirmed by mass spectrometry, and test by analytical HPLC found peptides to be greater than 95% pure.

Before attempting the coupling of the peptide and bipyridyl compound, two model compounds were created, one by forming the diamide with two moles of glycine benzyl ester, the other by using the alanine benzyl ester. In both cases, amidation was successful (approximately 70% yield in both cases). However, attempted condensation between 8-mer $\text{H}_2\text{N-GGGLMVGG-OH}$ and bipyridine diacid chloride **4** was unsuccessful, returning only starting material and slow hydrolysis of **4** to diacid **3**.

Synthesis of a Spin-Labelled Congo Red Derivative. The central piece of the Congo red derivative was made via commercially available 4,4'-dinitro-2-biphenylamine **6**. Reaction with NaNO_2/CuI in sulfuric acid afforded the iodinated biphenyl compound **7**, which on treatment with CuCN in refluxing DMSO gave the cyano compound **8**. Simultaneous reduction of the cyano and nitro groups to compound **10** via hydrogenation proved impossible, giving the diamine **9** with several impurities at pressures of up to 55 psi. The diamine was also obtained by treatment of **8** with KBH_4/CuCl .⁸ Refluxing of the diamine

Scheme 2



with LiAlH_4 in THF overnight successfully gave the triamine **10**. For attachment of the nitroxide spin label to the central core, commercially available spin label **11** was treated with ethyl chloroformate to form the anhydride according to a literature procedure,⁹ which upon addition to a solution of the triamine formed the spin-label derivatized central core **12**. Finally, diazotization of spin label **12** by a standard procedure gave compound **13**. Mass spectrometry to date has been inconclusive for compounds **12** and **13**, giving no $\text{M}+\text{H}$ peak but a series of smaller peaks corresponding to a diazotized naphthyl group in **13**.

Future Directions

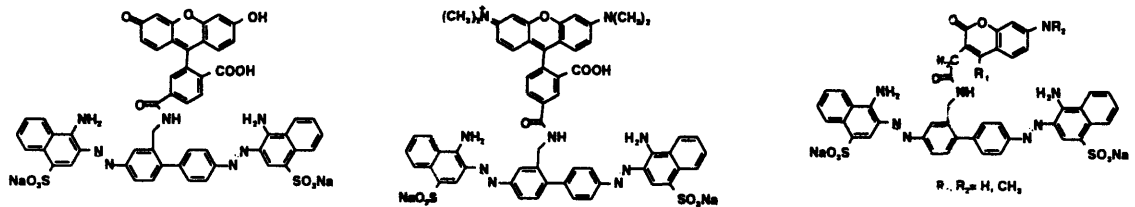
1) β -Sheet Nucleator. After synthesis of compounds **5** and **6**, obviously the next step would be to determine if such compounds are able to affect the aggregation rate of the A β peptide, as measured by our aggregation assay,¹⁰ or through the assay of Teplow.¹¹ Since both the 7- and 8-amino acid peptides have considerable water solubility, additional amino

acids in the $\beta(34-42)$ sequence could be added to find the maximum length of the A β peptide before solubility is appreciably affected. Other hydrophobic sequences, such as poly-valine or poly-phenylalanine, have also been suggested for their potential ability to bind to the β -amyloid fibril.

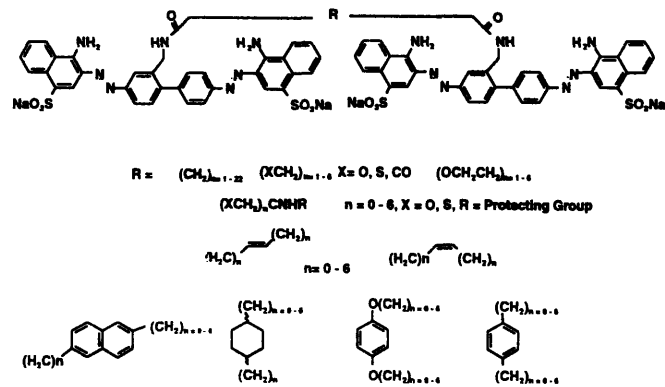
2) Spin-Labelled Congo Red. The Congo red assay has been developed by several laboratories^{1,12} The fibrils of the C-terminal peptide $\beta(34-42)$ have been determined by previous work to exhibit most of the properties of full-length $\beta(1-42)$ fibrils when stained with Congo red, and is amenable to solid-state NMR studies.¹³ This shorter peptide could be easily used for ESR studies to elucidate the structure of the bound CR-amyloid fibril, although extrapolations of binding modes to full-length $\beta(1-42)$ may not be completely analogous due to the absence of possible binding sites. For example, amino acids 12 to 15 have been suggested as a possible binding site for Congo red.¹⁴ In addition, the above synthesis lends itself easily to the derivatization of other aromatic biphenyl azo dyes. For example, Chrysamine G, which has also been used as an amyloid stain, is easily derived from a similar synthesis to the one outlined for Congo red, with salicylic acid replacing 4-amino-1-naphthalene sulfonic acid in the final diazotization step (see Scheme 3). Such a compound would conceivably give us further information regarding binding of such molecules to amyloid fibrils.

Ongoing research in our labs has used compound **10** as the precursor for an entire family of Congo red and Chrysamine G analogs (see Figure 2). In addition, another dye-binder has been created using 4-hydroxy-1-naphthalene sulfonic acid instead of 4-amino-1-naphthalene sulfonic acid as the naphthyl portion of the dye (W. Zhen and M. Anguiano, unpublished data). These compounds could be the first generation of a series of aromatic dye analogs whose affinity for various amyloid fibrils, such as those predominantly derived from A $\beta(1-42)$ or A $\beta(1-43)$, another variant form of long A β , could be tuned by

Amyloid Binding Fluorescence Probes



Amyloid Staining Agents



Amyloid Diagnostic Agents

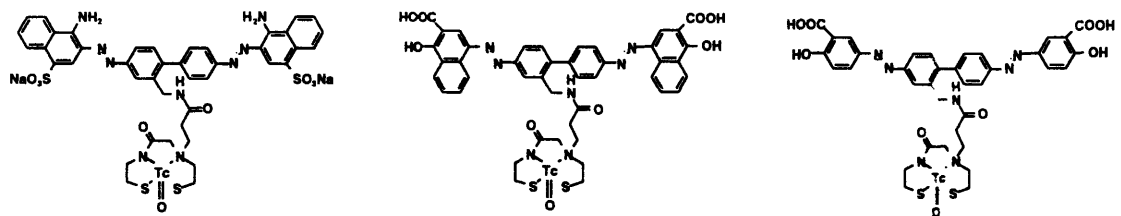
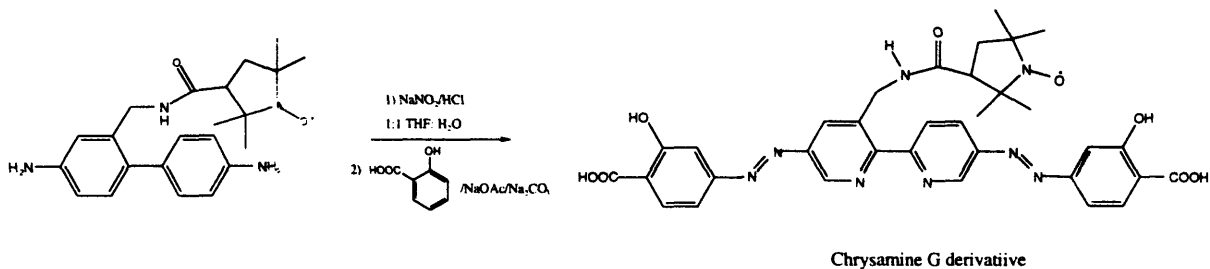


Figure 2: Some potential amyloid diagnostic and staining targets based on Congo Red and Chrysin

Scheme 3



modification of the naphthyl and/or biphenyl moieties.

Experimental

2-Iodo-4,4'-dinitrobiphenyl (7). 5,5'-Dinitro-2-biphenylamine (10.03 g, 38.7 mmol) was dissolved in concentrated H_2SO_4 (40 ml) with stirring. Separately, NaNO_2 (3.52 g) was mortar ground and added in portions to H_2SO_4 (25 ml) at 5°C , with minimum evolution of nitrogen. The resulting slush was pipetted into the amine solution at 0°C , followed by 85% phosphoric acid (95 ml) added by addition funnel over 1 hour, maintaining the temperature below 10°C throughout. The solution was then allowed to warm to room temperature over 2 hours with constant stirring. Due to the viscosity of the solution, occasional hand agitation was necessary. After 2 hours, the solution was dumped into 500 ml of ice water and stirred until the solution was homogenous, when urea (7.53 g) was added to destroy excess nitrous acid. Finally, a solution of KI (15.26 g) in water (100 ml) was added by pipette and the solution stirred for 15 minutes. The resulting solution was filtered, and the solid redissolved in CH_2Cl_2 and extracted with aqueous sodium bisulfite. The organic layer was collected, dried with MgSO_4 , concentrated and chromatographed in 1:1 hexane: CH_2Cl_2 to yield product **7** (11.560 g, 80.9%). ^1H NMR(300 MHz, CDCl_3): δ 8.83 (d, 1 H, $J = 2.4$ Hz), 8.35 (d, 2 H, $J = 8.4$ Hz), 8.30

(dd, 1 H, $J_1 = 8.4$ Hz, $J_2 = 2.4$ Hz), 7.55 (d, 2 H, $J = 8.4$ Hz), 7.48 (d, 1 H, $J = 8.4$ Hz); ^{13}C NMR(300 MHz, CDCl_3): δ 150.44(C-4), 148.09(C-4), 147.82(C-6), 147.50(C-1), 134.50(C-3), 129.88(C-2, C-6), 124.25(C-1), 123.58(C-3, C-5), 123.16(C-5), 96.95(C-2).

2-Cyano-4,4'-dinitrobiphenyl (8). Compound **7** (11.56 g, 31.2 mmol) and CuCN (16.80 g, .188 mol) were placed under argon, dissolved in anhydrous DMSO (50 ml) and refluxed at 190° C for 2 hours. The reaction mixture was poured into concentrated NH_4Cl and allowed to cool to room temperature, then filtered. The solid was redissolved in THF, and extracted with THF: CH_2Cl_2 and water. The organic phase was dried with MgSO_4 , concentrated to a beige solid, and chromatographed (20:80 THF:hexane) to give an off-yellow solid **8** (5.97 g, 71%). ^1H NMR(300 MHz, CDCl_3): δ 8.69 (d, 1 H, $J = 2.4$ Hz), 8.58 (d, 1 H, $J = 2.4$ Hz), 8.42 (dd, 2 H, $J_1 = 8.4$ Hz, $J_2 = 2.4$ Hz), 7.78 (m, 3 H); ^{13}C NMR(300 MHz, CDCl_3): δ 148.67(C-4), 148.45(C-4), 147.46(C-1), 141.85(C-1), 131.27(C-6), 129.79(C-2, C-6), 128.87(C-5), 127.64(C-3), 124.25(C-3, C-5), 115.77(CN), 112.97(C-2).

4,4'-Diamino-2-cyanobiphenyl (9): Primary route. Compound **8** (1.39 g, 5.16 mmol) was placed in MeOH and 10% Pd/C (100 mg) in EtOH (5 ml) was added. The solution was hydrogenated in a Parr apparatus for 24 hours at 55 psi. TLC in 5:95 MeOH: CH_2Cl_2 showed complete disappearance of starting material with appearance of a new spot at $R_f = 0.4$. Filtration of the solution and concentration gave a yellow-orange product which was carried over to the next step.

4,4'-Diamino-2-cyanobiphenyl (9): Secondary route. Compound **8** (975 mg, 3.62 mmol) was placed under argon and dissolved in anhydrous MeOH (30 ml) with sonication. Anhydrous CuCl (1.24 g, 12.53 mmol) was added followed by KBH_4 (1.54 g, 28.54 mmol) in portions. Upon addition of the borohydride, a black precipitate formed and the solution darkened to green. The solution was allowed to stir for 1 hour, then concentrated to remove MeOH. The resultant was redissolved in H_2O , filtered and the

solution extracted with EtOAc. The organic layer was dried with MgSO_4 , concentrated to a yellow solid, and chromatographed (1:99 MeOH: CH_2Cl_2) to give a red solid, **9** (588 mg, 77.6%). ^1H NMR(300 MHz, DMSO- d_6): δ 7.66-7.59 (m, 3 H), 7.37-7.32 (m, 2 H), 7.10-7.04 (m, 2 H), 5.98 (s, 2 H), 5.69 (s, 2 H); ^{13}C NMR(300 MHz, DMSO- d_6): δ 148.37(C-4), 147.53(C-4), 132.90(C-6), 130.39(C-6), 129.06(C-2), 126.13(C-1), 125.89(C-1), 119.90(C-5), 119.13(C-5), 117.14(C-2), 114.47(C-3), 113.87(C-3), 109.51 (CN).

4,4'-Diamino-2-(aminomethyl)biphenyl (10). In separate flasks, LiAlH_4 (369 mg, 6.255 mmol) and compound **9** (115 mg, .550 mmol) were placed under argon and dissolved in dry THF (20 ml). The solution of **9** was added dropwise to the LAH slurry, and the combined solutions refluxed for 19 hours at 110° C. After 19 hours, the solution was cooled to RT, and water followed by 5% NaOH added to neutralize excess hydride. The resultant was filtered and extracted with hexane. The aqueous layer was kept, acidified to pH 4, extracted with CH_2Cl_2 , and the resulting aqueous layer lyophilized to an orange powder, the triamine **10** (86.8 mg, 74%). ^1H NMR (300 MHz, DMSO- d_6): δ 6.96 (d, 2 H), 6.81 (d, 1 H), 6.73 (s, 1 H), 6.60 (d, 2 H), 6.47 (dd, 1 H), 4.94 (4 H), 3.57 (s, 2 H), 3.17 (2 H); ^{13}C NMR (300 MHz, DMSO- d_6): δ 147.06(C-4), 146.74(C-4), 130.18(C-1), 130.06(C-1), 129.84(C-2, C-6), 129.66(C-3, C-5), 129.31(C-6), 129.23(C-2), 113.72(C-3), 112.26(C-5), 67.08(CH_2).

3-[2-(amidomethyl)-4,4-diaminobiphenyl]-2,2,5,5-tetramethyl-1-pyrrolidinyloxy, free radical (12). Spin label 3-Carboxy PROXYL (**11**) (93.5 mg, .502 mmol) was dissolved in dry THF, and freshly distilled ethyl chloroformate (48 mL) was added dropwise. The solution was stirred at room temperature for 3 hours, until TLC (10:90 methanol:dichloromethane) confirmed consumption of starting material. A solution of **10** (107 mg, .502 mmol) in dry THF (10 ml) was then added, and Et_3N (70 ml) finally added dropwise. The solution was left to stir overnight, then concentrated. Chromtography followed by mass spectrometry gave a yellow compound believed to be **12**.

3-[2-(amidomethyl)-3,3'-[4,4'-biphenylenebis(azo)]bis[4-amino-1-naphthalene sulfonic acid]-2,2,5,5-tetramethyl-1-pyrrolidinyloxy, free radical (13). To an ice-cooled solution of **12** (23.9 mg, .0628 mmol) in 1:1 THF/H₂O (4 ml) was added dropwise 10% aqueous HCl (280 ml) followed by an ice-cooled solution of NaNO₂ in H₂O (64.7 mg in 280 ml). After 15 minutes at 0^o C, the solution was added dropwise to a solution of 4-amino-1-naphthalene sulfonic acid (74.5 mg, .334 mmol), sodium acetate trihydrate (245 mg, 1.80 mmol), and sodium bicarbonate (23.9 mg, .225 mmol) in H₂O (2 ml) at 0^o C. The solution immediately turned red and was allowed to stir for 1 hour. TLC (50:50 methanol:dichloromethane) showed a new spot. Material was immediately concentrated, redissolved, and column chromatography (dichloromethane, then 10:90 to 50:50 methanol:dichloromethane) gave a red solid believed to be compound **13** (15%). Mass spec(FAB-, glycerol matrix):m/z = 205, 221, 222, 243, 249, 265, 275, 281, 357.

References for Chapter II

- (1) Cooper, J.H. *Lab. Invest.* **1974** *31* , 232-238
- (2) Ashburn, T.T., The Molecular Basis of Pancreatic Amyloid Deposition in Type II Diabetes and the Binding of Congo Red to Amyloid, *Ph.D. Thesis*, **1995**.
- (3) Han, H.; Cho, C.-G.; Lansbury, P.T.J. *J. Am. Chem. Soc.* **1996** ,
- (4) LaBrenz, S.R.; Kelly, J.W. *J. Am. Chem. Soc.* **1995** *117* , 1655-1656
- (5) Schneider, J.P.; Kelly, J.W. *J. Am. Chem. Soc.* **1995** *117* , 2533-2546
- (6) Park, T.K., Molecular Recognition of Nucleic Acid Components, *Ph.D. Thesis, Massachusetts Institute of Technology*, **1992**.
- (7) Case, F.H. *J. Am. Chem. Soc.* **1946** *68* , 2574-2577
- (8) He, Y.; Zhao, H.; Pan, X.; Wang, S. *Synth. Comm.* **1989** *19* , 3047-3050
- (9) Erlich, R.H.; Starkweather, D.K.; Chignell, C.F. *Mol. Pharm.* **1972** *9* . 61-73
- (10) Jarrett, J.T.; Berger, E.P.; Lansbury, P.T., Jr. *Biochem.* **1993** *32* , 4693-4697
- (11) Lomakin, A.; Chung, D.S.; Benedek, G.B.; Kirschner, D.A.; Teplow, D.B. *Proc. Natl. Acad. Sci. USA* **1996** *93* , 1125-1129
- (12) Puchtler, H.; Sweat, F.; Levine, M. *J. Histochem. Cytochem.* **1962** *10* , 355-364
- (13) Lansbury, P.T., Jr.; Costa, P.R.; Griffiths, J.M.; Simon, E.J.; Auger, M.; Halverson, K.J.; Kocisko, D.A.; Hendsch, Z.S.; Ashburn, T.T.; Spencer, R.G.S.; Tidor, B.; Griffin, R.G. *Nature Struct. Bio.* **1995** *2* , 990-998
- (14) Elhaddaoui, A.; Pigorsch, E.; Delacourte, A.; Turrell, S. *J. Mol. Struct.* **1995** , 363-369

Appendix

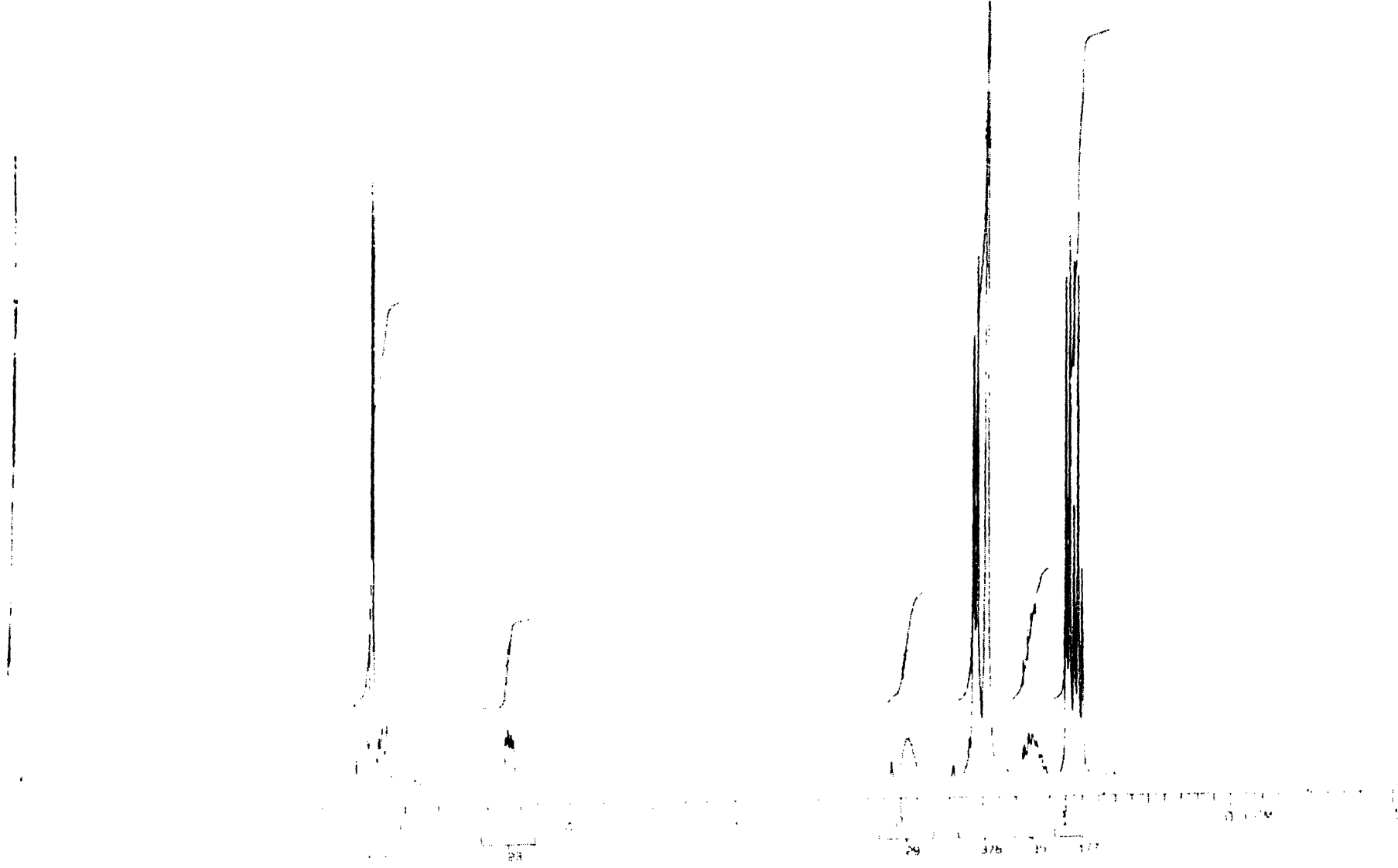
NMR (300 MHz, DMSO or CDCl₃):

| | |
|--|----|
| Boc-L-isoleucyl-L- α -lactic acid benzyl ester (¹ H) | 36 |
| Boc-L-isoleucyl-L- α -lactic acid benzyl ester (¹³ C) | 37 |
| Boc-L-isoleucyl-L- α -lactic acid (¹ H) | 38 |
| Boc-L-isoleucyl-L- α -lactic acid (¹³ C) | 39 |
| 2-Iodo-4,4-Dinitrobiphenyl (¹ H) | 40 |
| 2-Iodo-4,4-Dinitrobiphenyl (¹³ C) | 41 |
| 2-Cyano-4,4-Dinitrobiphenyl (¹ H) | 42 |
| 2-Cyano-4,4-Dinitrobiphenyl (¹³ C) | 43 |
| 4,4-Diamino-2-Cyanobiphenyl (¹ H) | 44 |
| 4,4-Diamino-2-Cyanobiphenyl (¹³ C) | 45 |
| 4,4-Diamino-2-(aminomethyl)biphenyl (¹ H) | 46 |
| 4,4-Diamino-2-(aminomethyl)biphenyl (¹³ C) | 47 |

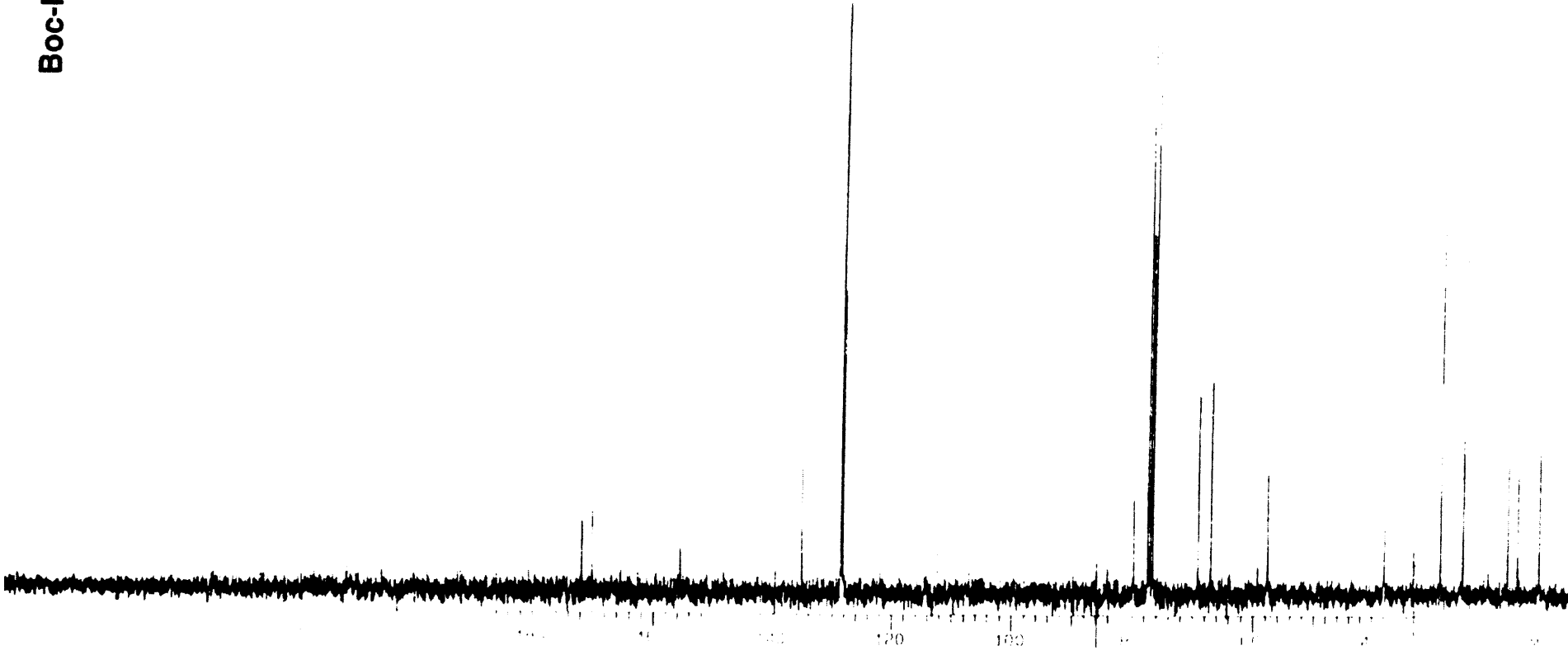
Mass Spectrometry

| | |
|---|----|
| 3-[2-(amidomethyl)-3,3'-[4,4'-biphenylene bis(azo)]bis[4-amino-1-naphthalene sulfonic acid]-2,2,5,5-tetramethyl-1-pyrrolidinyloxy, free radical | 48 |
|---|----|

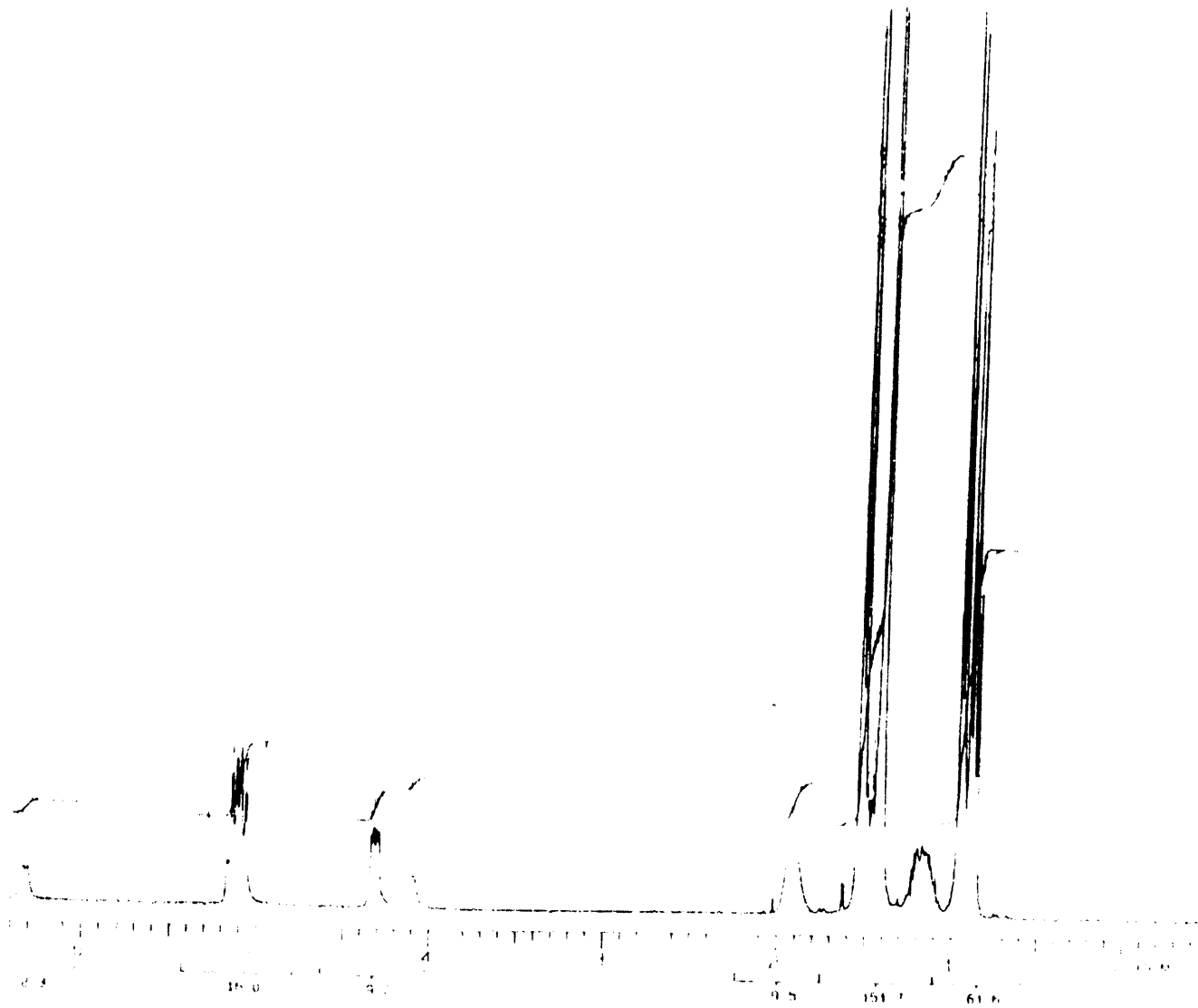
Boc-Ile-Lac-OBn



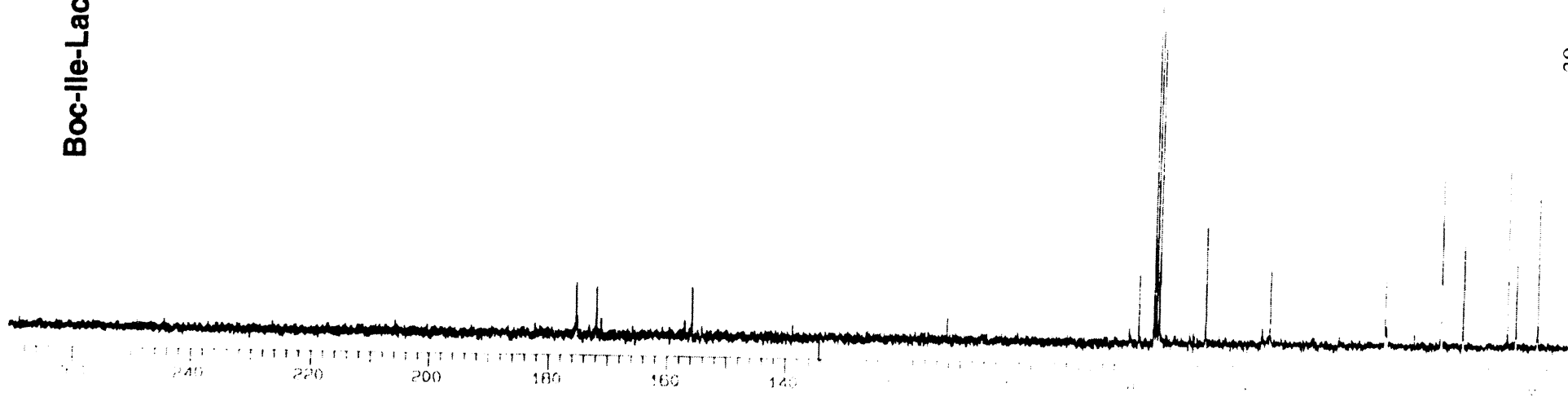
Boc-Ile-Lac-OBn



Boc-Ile-Lac-OH



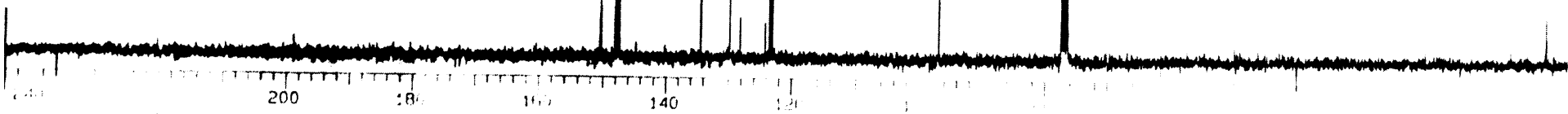
Boc-Ile-Lac-OH



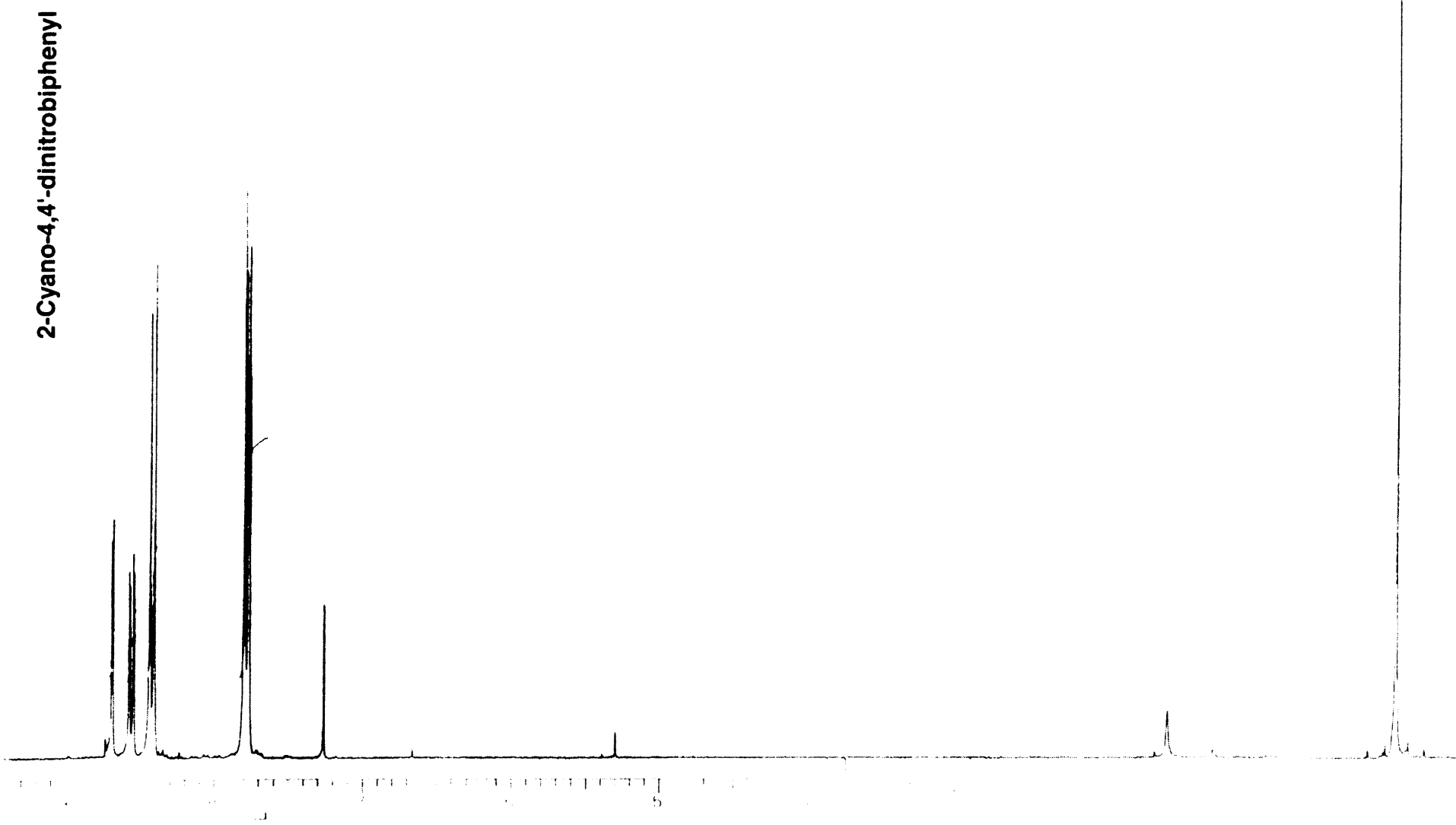
2-Iodo-4,4'-dinitrophenyl



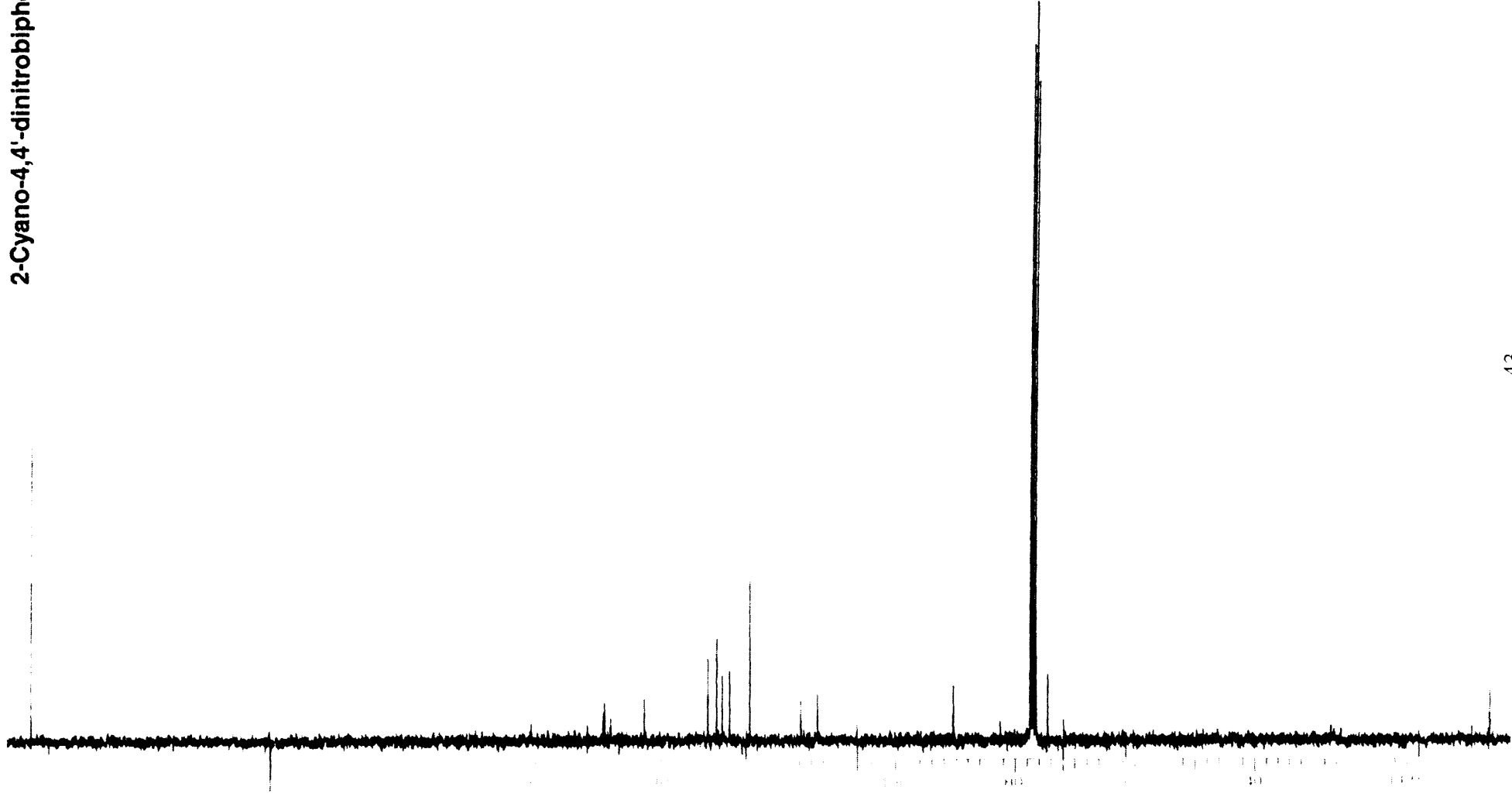
2-Iodo-4,4'-dinitrobiphenyl



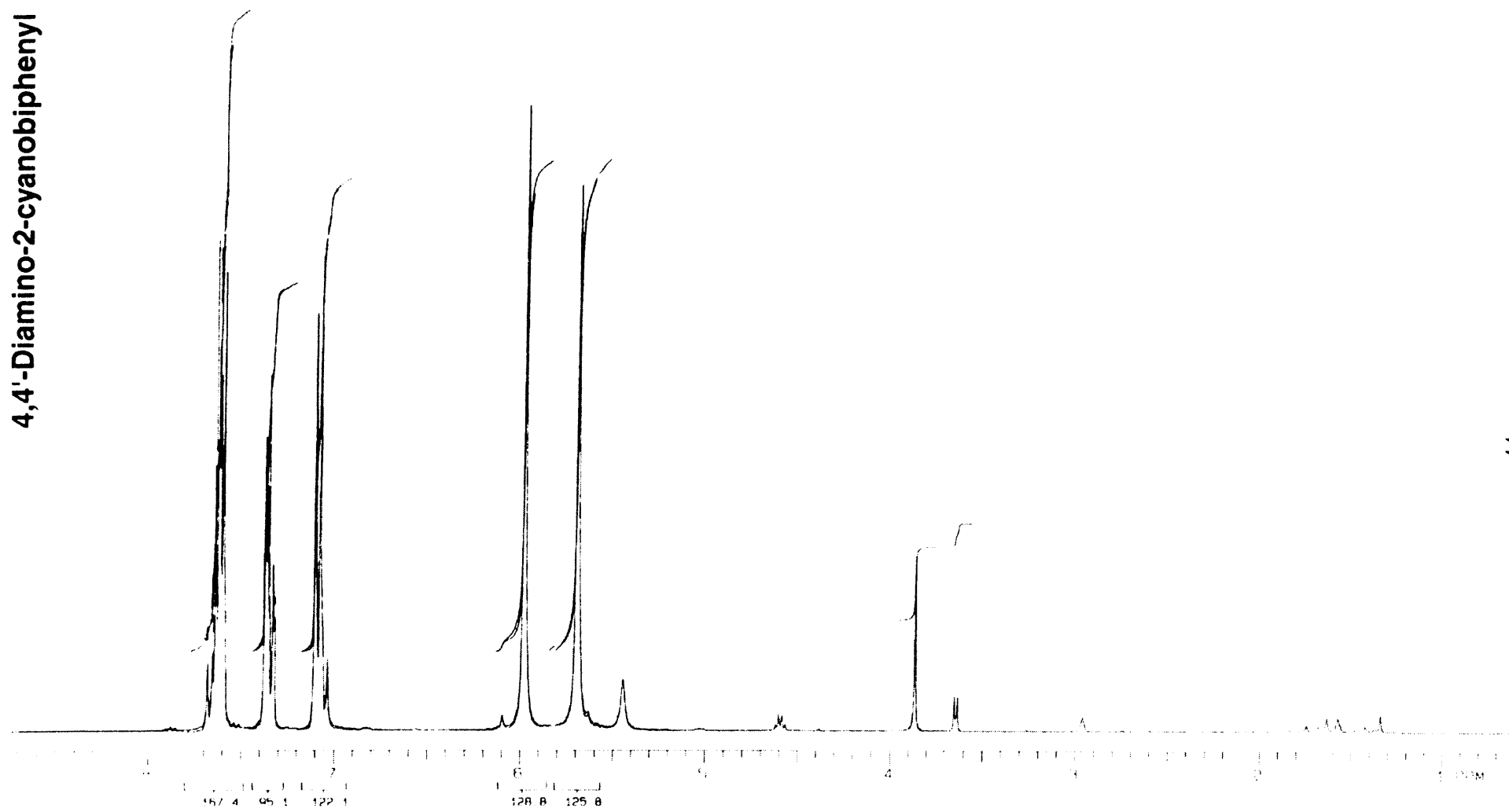
2-Cyano-4,4'-dinitrophenyl



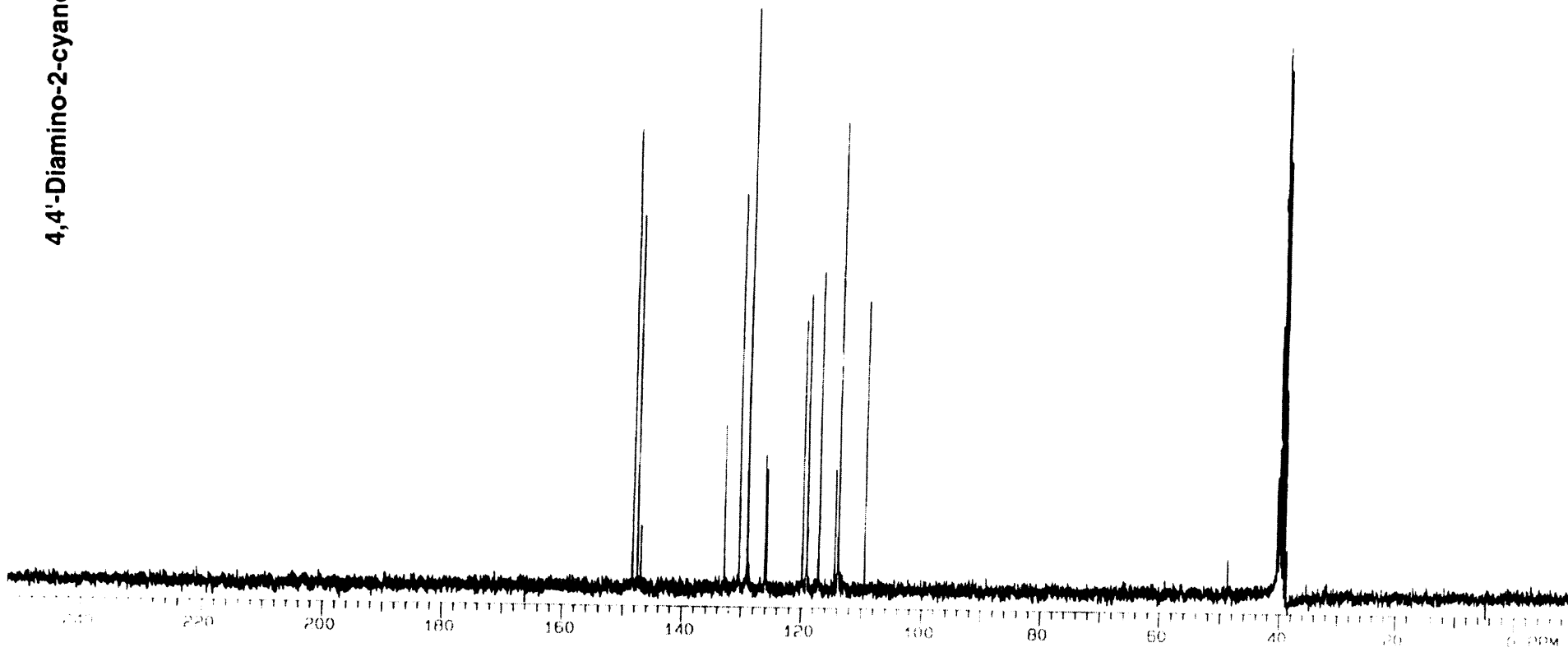
2-Cyano-4,4'-dinitrophenyl



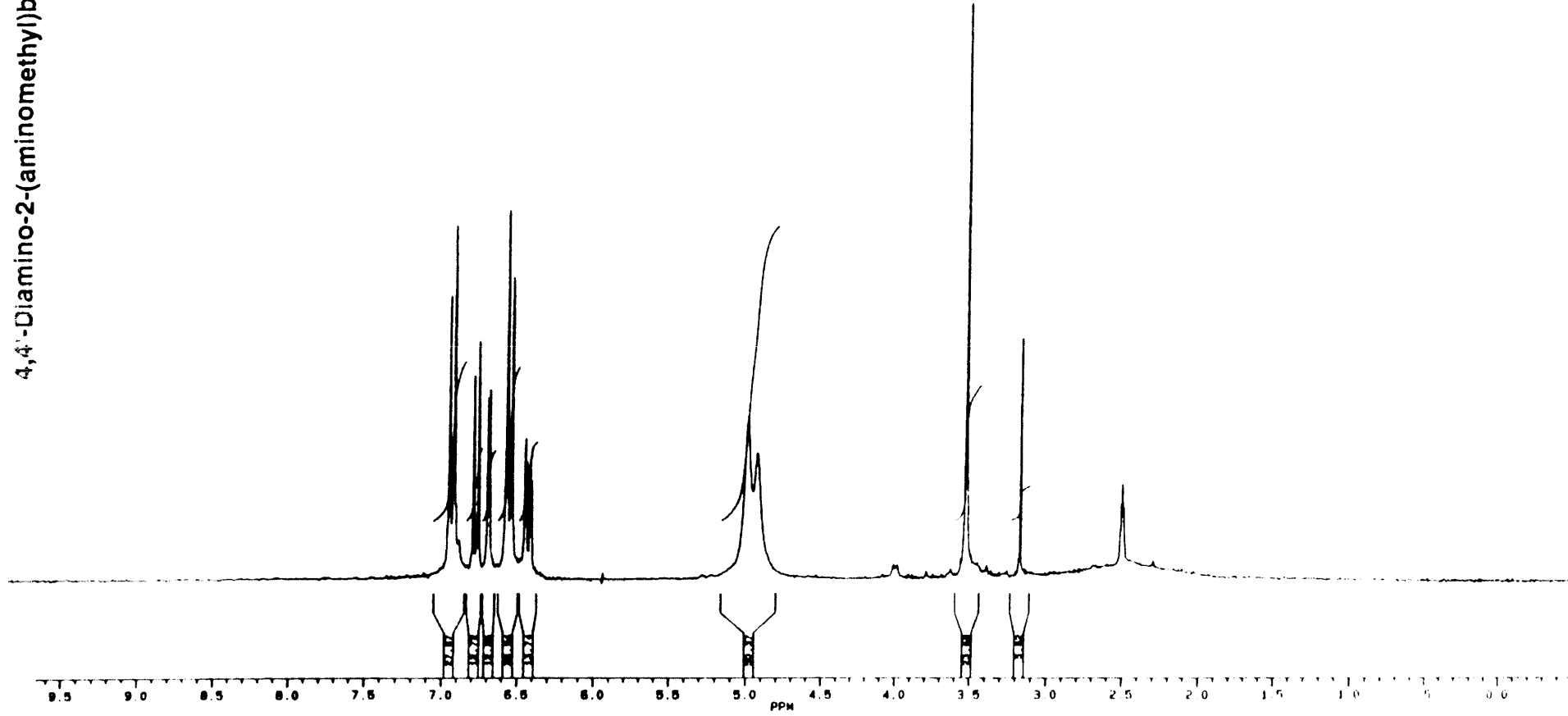
4,4'-Diamino-2-cyanobiphenyl



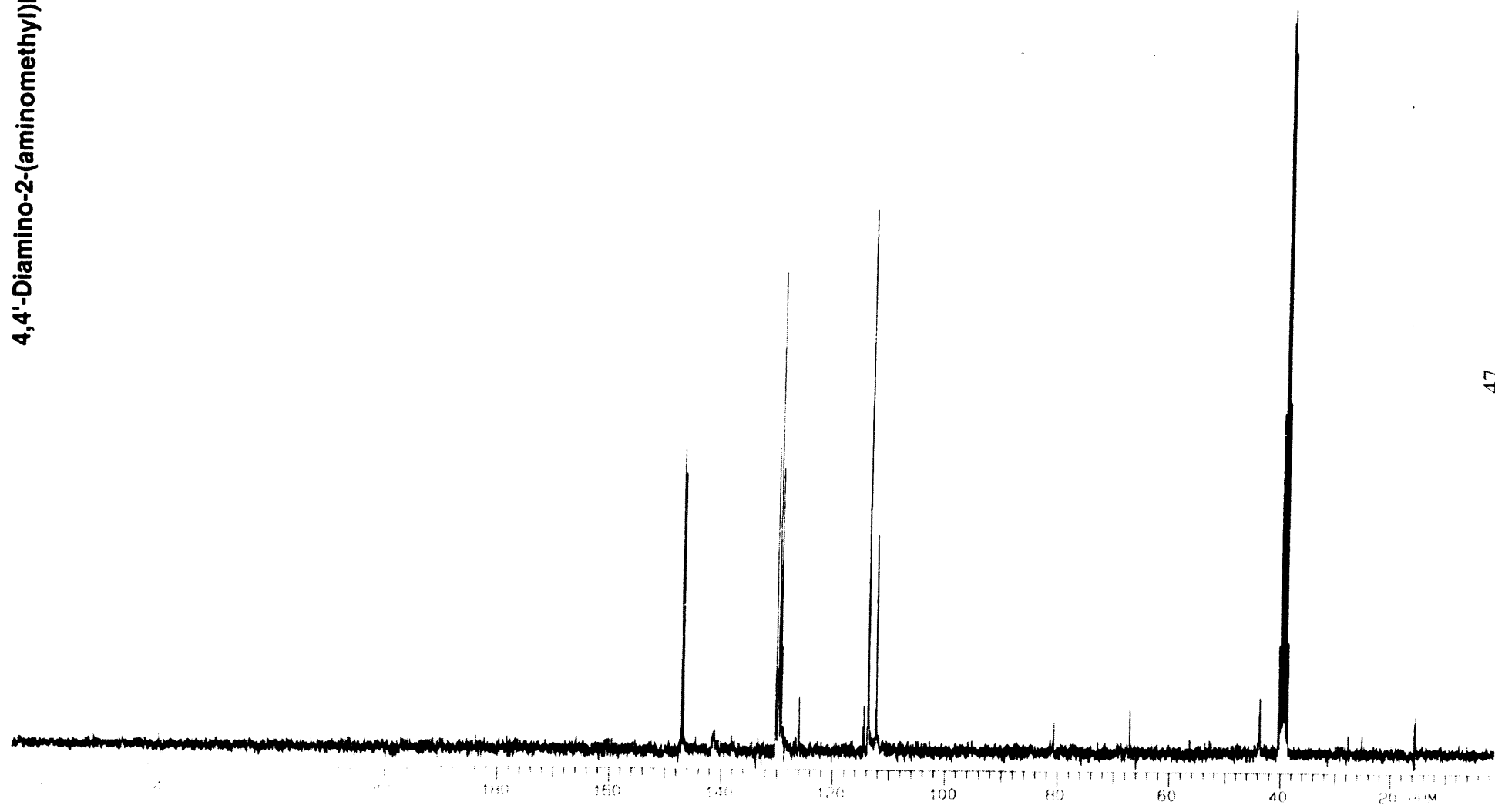
4,4'-Diamino-2-cyanobiphenyl



4,4'-Diamino-2-(aminomethyl)biphenyl



4,4'-Diamino-2-(aminomethyl)biphenyl



[Mass Spectrum]

Data : ng001HIM

Date : 05-May-97 09:59

Sample: CLM-275

Note : neg ion Glycerol

Inlet : Direct

Ion Mode : FAB-

Spectrum Type : Regular [MF-Linear]

RT : 0.67 min

Scan# : (2,11)

Temp : 0.0 deg.C

BP : m/z 15.0000

Int. : 1.80

Output m/z range : 190.0000 to 1000.0000

Cut Level : 0.00 %

